Predictions of Slat Noise from the 30P30N at High Angles of Attack using Zonal Hybrid RANS-LES

Jeffrey Housman, Gerrit-Daniel Stich, and Cetin Kiris
Computational Aerosciences Branch
NASA Ames Research Center

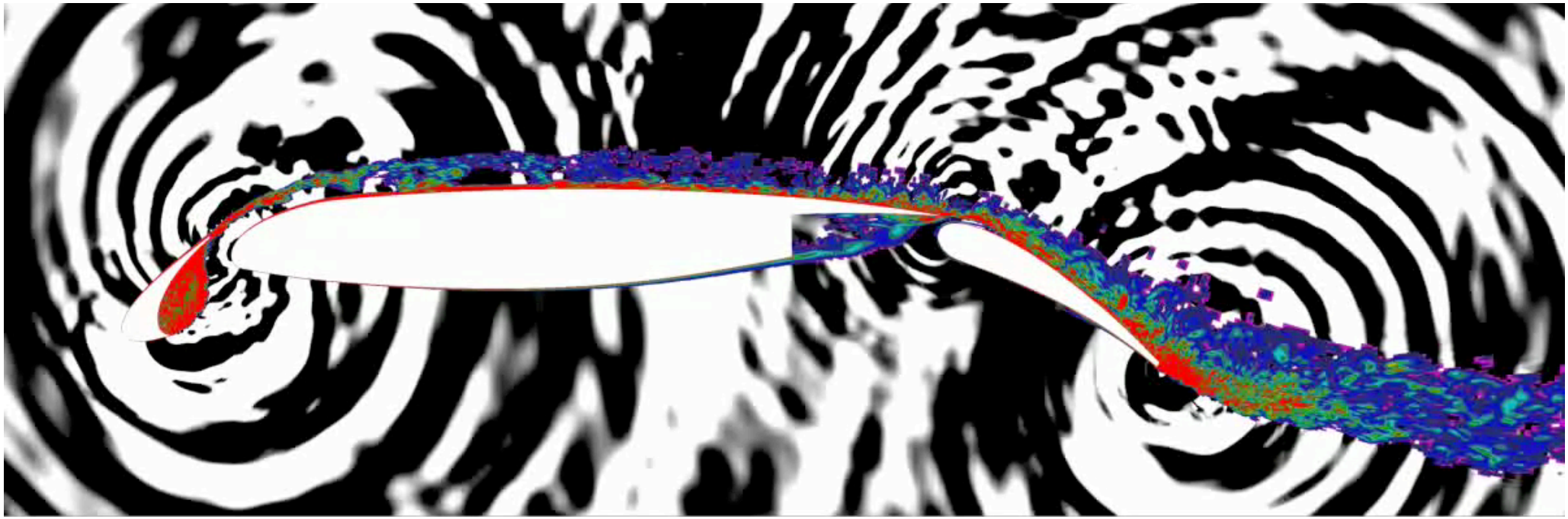

AIAA-2019-2438

Outline

- Introduction
- Problem Description
- Computational Methodology
- RANS Analysis
  - Overset grid system
  - Mesh Sensitivity
- Aeroacoustic Analysis
  - Flow-Field Visualization
  - Near-Field Results
  - Far-Field Results
- Summary

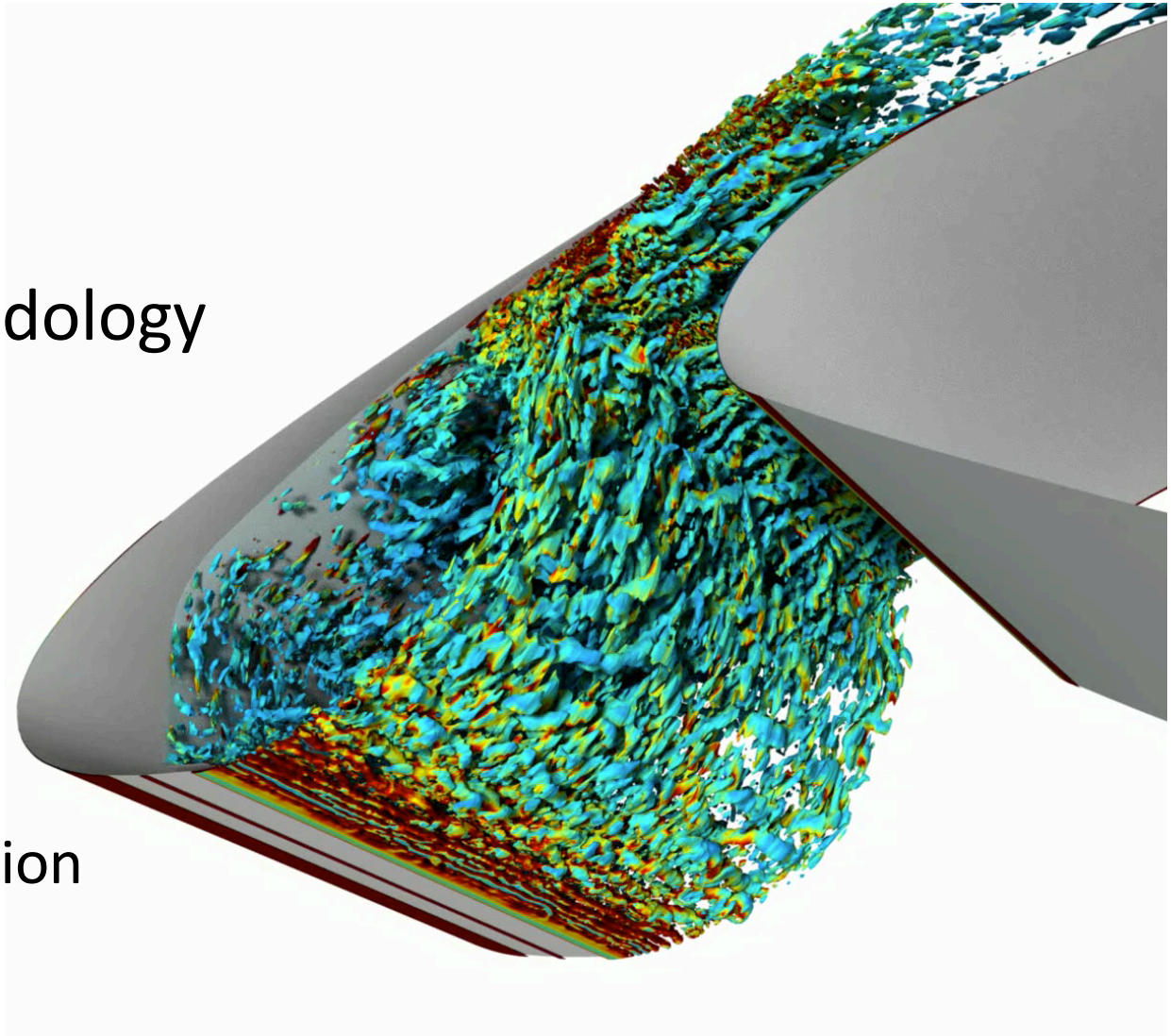

Iso-contour of Q-criteria colored by vorticity magnitude

Introduction

- Propulsion related aircraft noise has decreased substantially over the last decade resulting in a larger contribution of noise attributed to the airframe
- During landing, the noise generated by high-lift devices (such as slats) cause large amplitude broadband (and narrow band) sound waves

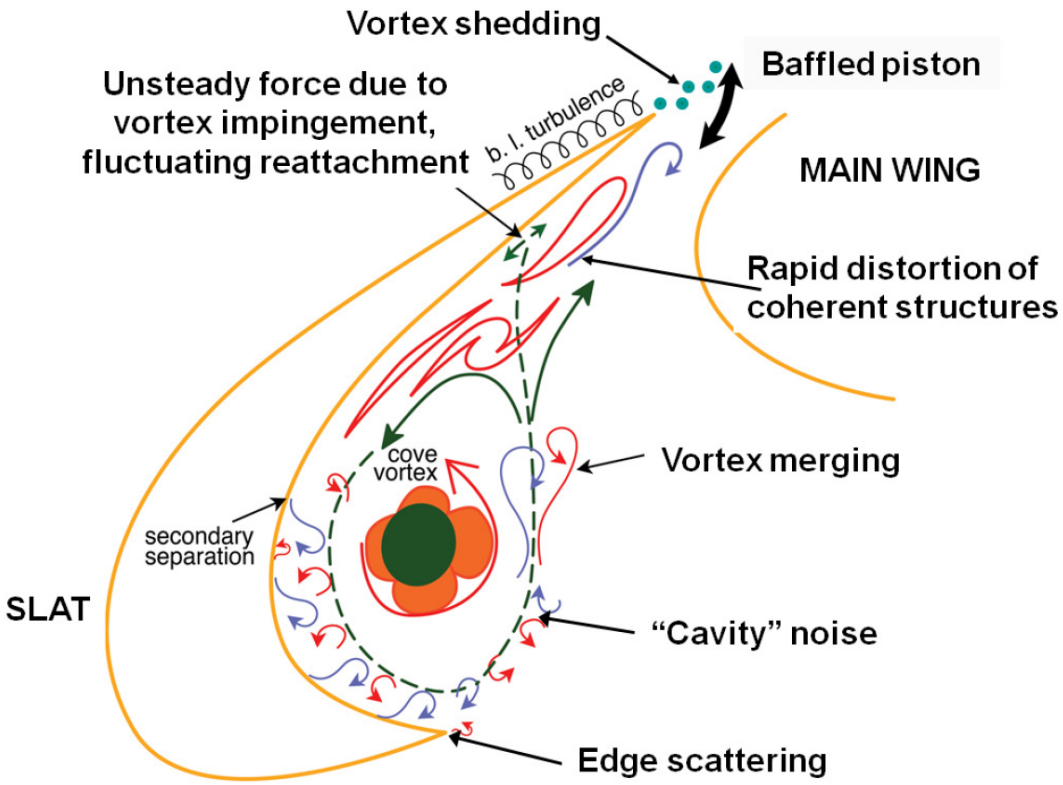

Diagram from BANC Workshop
Category 7 Problem Description

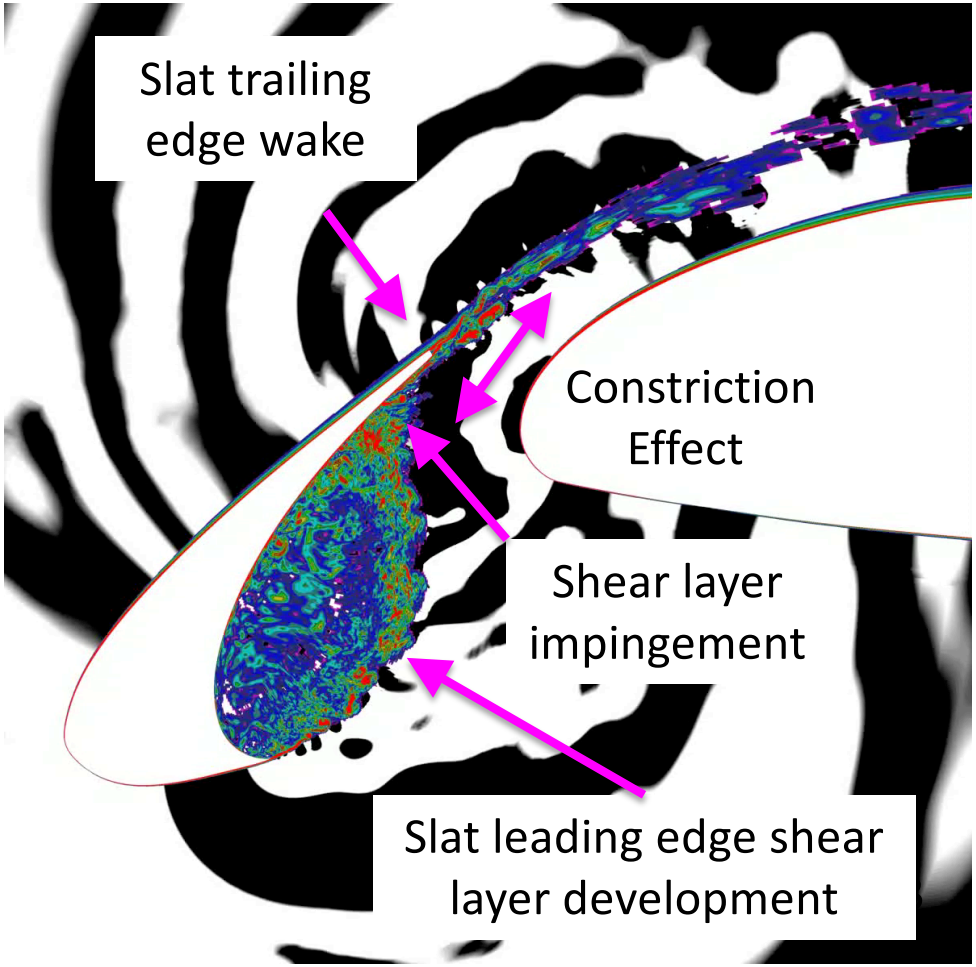

Introduction

- Starting in 2010 the AIAA has organized a series of workshops devoted to further the understanding of airframe noise, Benchmark Problems for Airframe Noise Computations (BANC)
- Category 7: *Slat Noise* targets the slat noise generated from the 30P30N 3-element airfoil designed by McDonnell-Douglas
- A detailed review can be found in ***AIAA-2015-2844***, Choudhari and Lockard

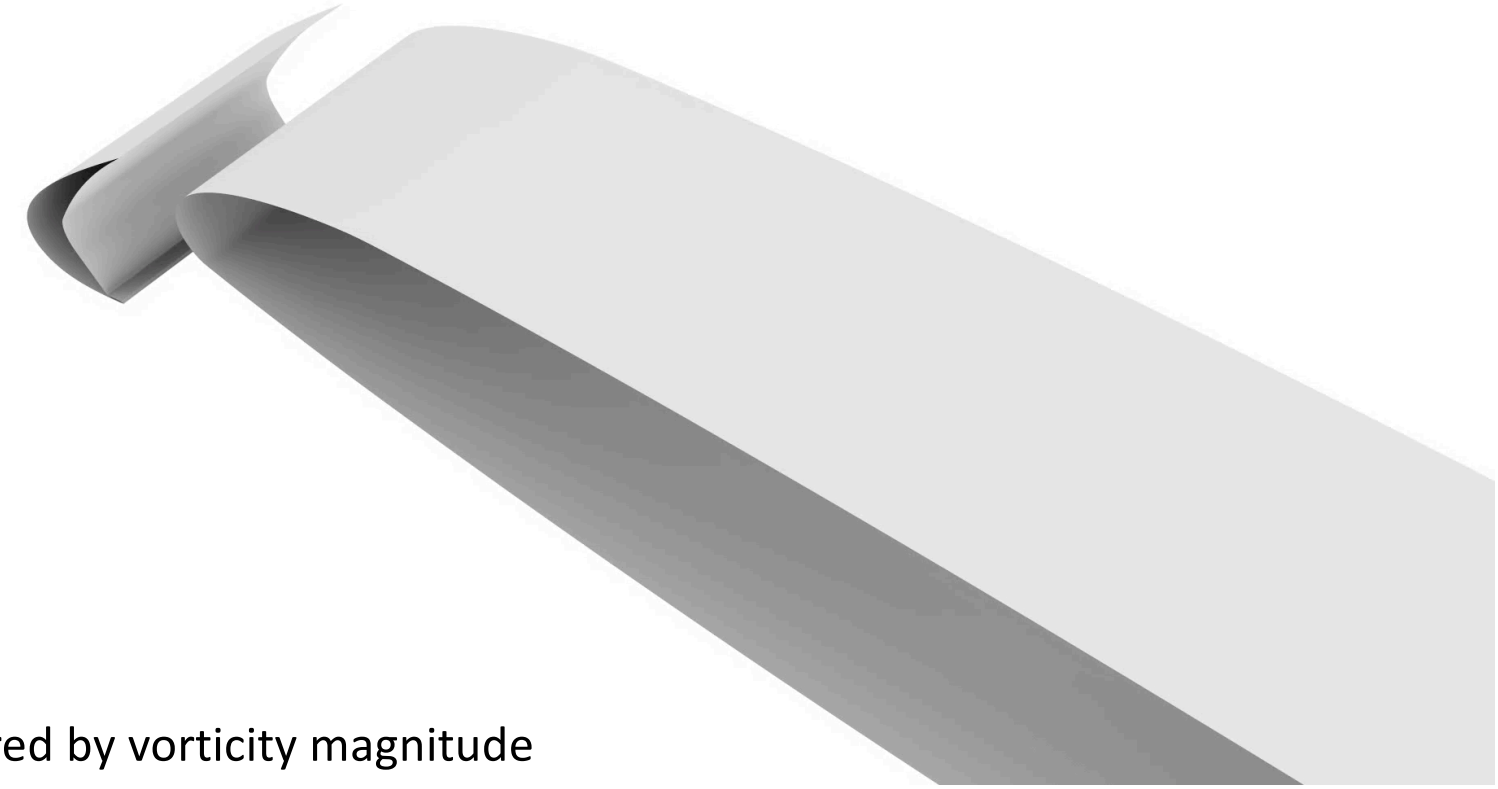

Particles colored by vorticity magnitude

Introduction

- The LAVA team has contributed to the category 7 slat noise problem at:
  - BANC-III: provided DDES simulations at two different mesh resolutions
  - BANC-IV: provided ZDES simulations at three different mesh resolutions using high-order accurate finite-difference scheme
  - BANC-V: provided ZDES simulations including three angles of attack

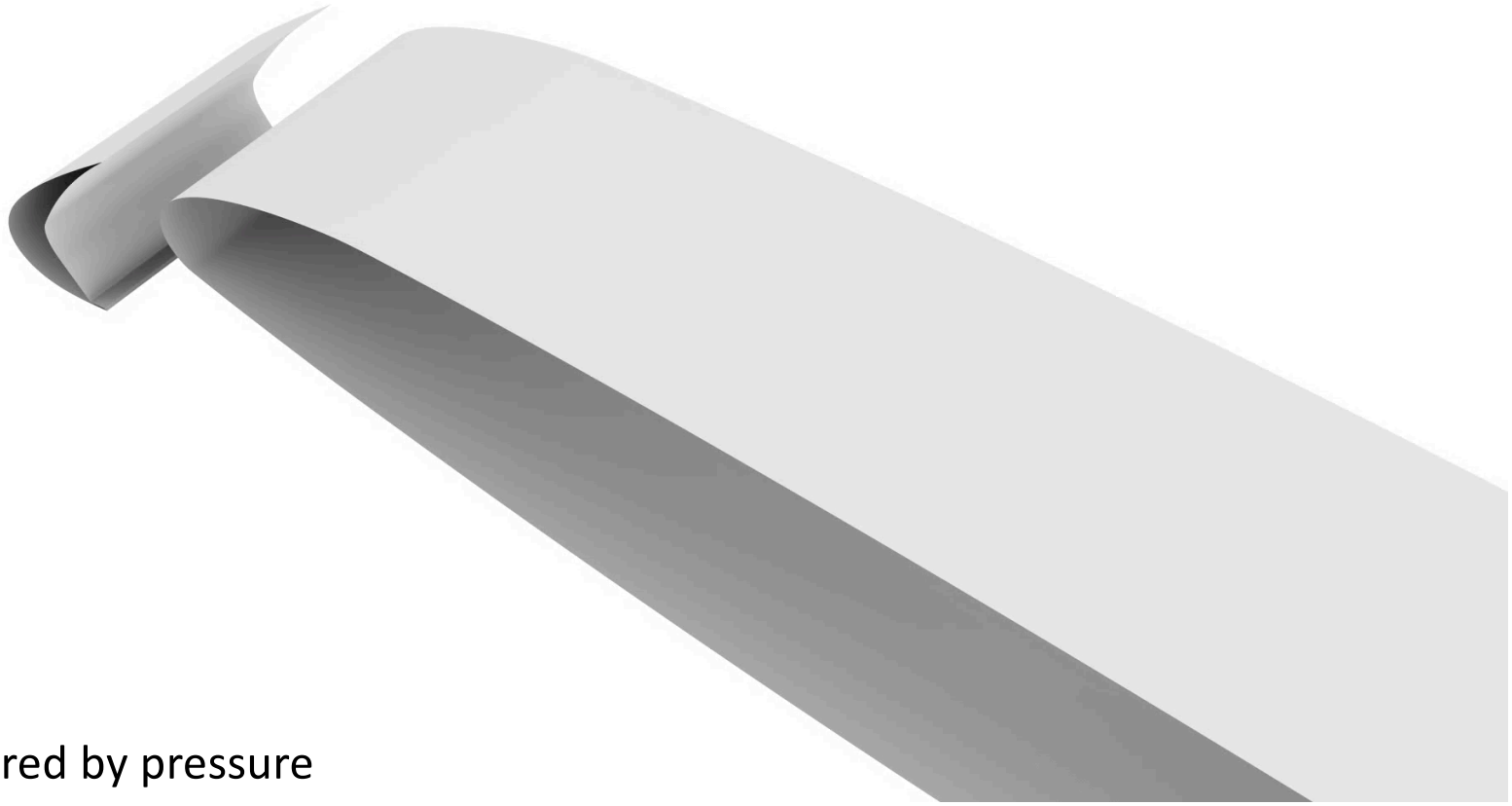

Particles colored by pressure

Problem Description

Geometric Model

30P30N Configuration F

- Stowed Chord c = 0.457 m
- Slat
  - Chord c_s= 0.15 c
  - Gap 2.95%
  - Overlap = -2.5%
- Flap
  - Chord = 0.3 c
  - Gap = 1.27%
  - Overlap = 0.25%

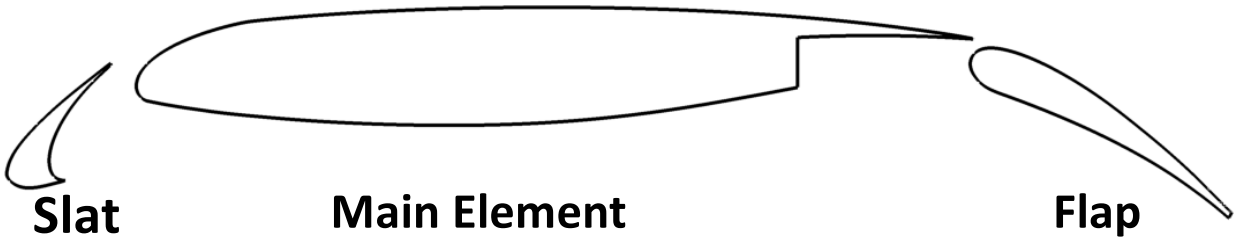

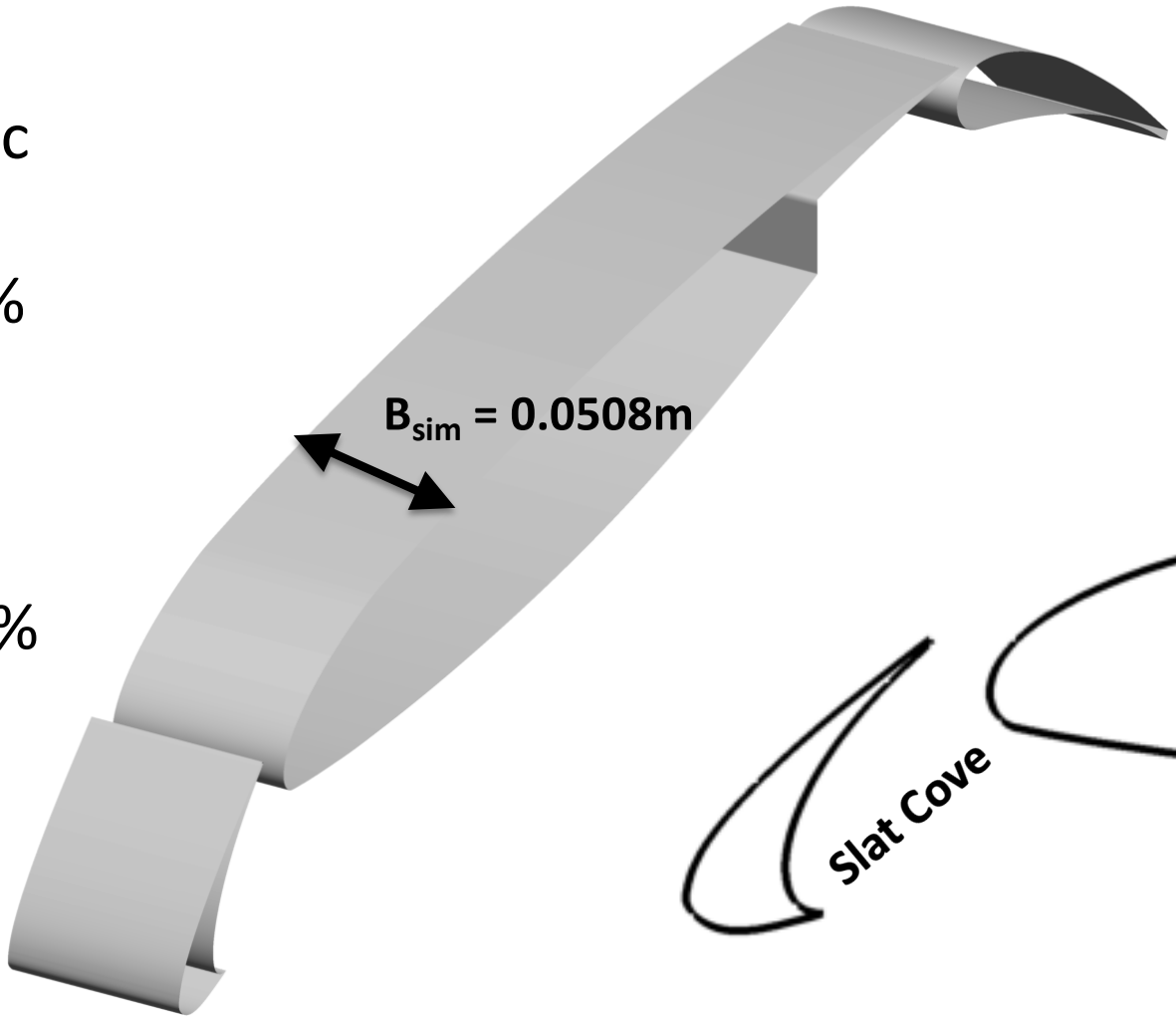

Problem Description

Conditions

- Mach = 0.17 (U_{ref} = 58 m/s)
- Re_C = 1.71 million
- AOA = 5.5°, 9.5°, and 14.0°

Simulation Procedure

- Steady-State RANS
- Time-accurate hybrid RANS-LES
  - Δt = 1 μs
  - 3 orders residual reduction at each time-step
  - 150K time steps

LAVA Framework

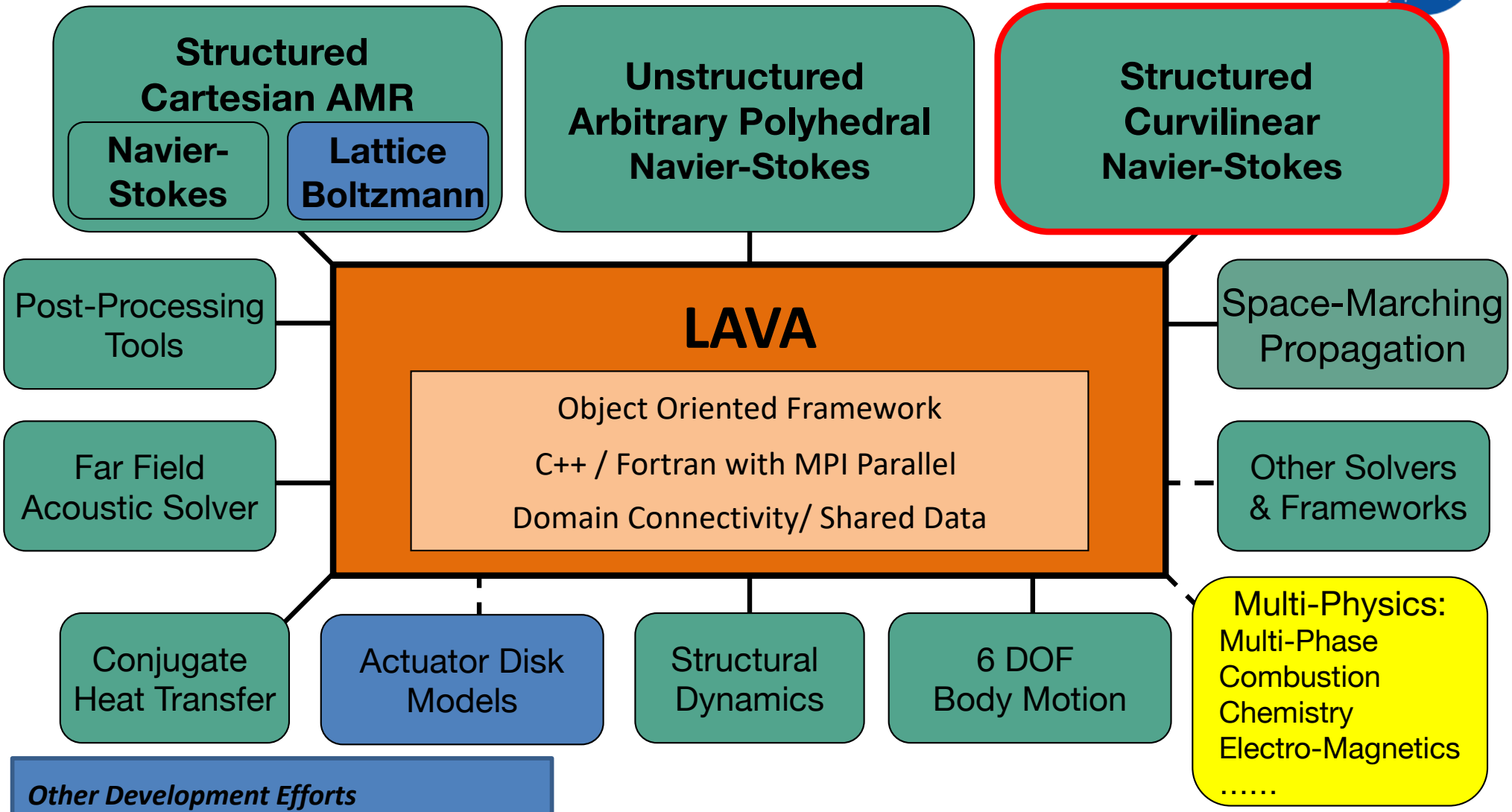

Other Development Efforts

- Higher order and low dissipation
- Curvilinear grid generation
- Wall modeling
- LES/DES/ILES Turbulence
- HEC (optimizations, accelerators, etc)

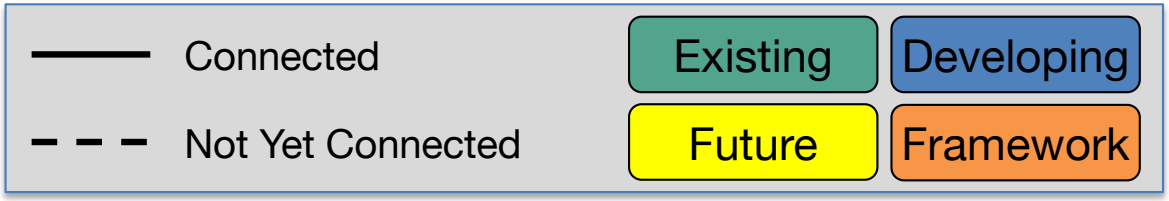

Kiris at al. AIAA-2014-0070 & AST-2016

Computational Methodology

3-D Structured Curvilinear Overset Grid Solver

- Zonal Detached Eddy Simulation (ZDES)
  - Spalart-Allmaras turbulence model for baseline RANS model
  - Near wall functions are removed when in LES mode
  - Cube-root of volume used for LES length scale
  - Introduced Mode 4 (pure LES mode)
- 4^{th} order Hybrid Weighted Compact Nonlinear Scheme (HWCNS) used for convective fluxes and metric terms
- 2^{nd} order accurate differencing used for time and viscous fluxes

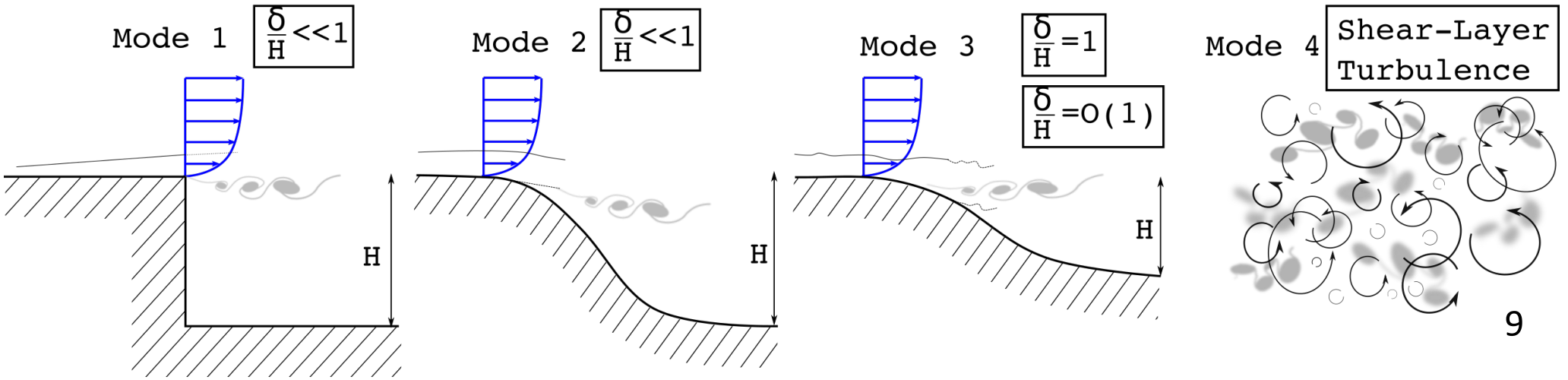

Computational Methodology

Structured Overset Grid Procedure

- Build initial coarse grid appropriate for RANS analysis, but with some intent on higher-fidelity modeling of the slat flow field
- Perform RANS based mesh convergence study (consistent family of uniformly refined meshes)
- Construct Hybrid RANS/LES grid from selected RANS mesh
  - Utilize spatially varying spanwise resolution for different regions
  - Select ZDES "Mode" for each zone (region)

NOTE:

In BANC-IV the intent was to model all noise sources of the 30P30N which required:

- Many grid points to capture the main element flap cove region and flap TE
- Utilized the same spanwise spacing throughout the grid system
- Utilized high-order accurate finite differencing schemes (6^{th} order and up to 8^{th} order in the spanwise direction)

This lead to an accurate simulation for the aeroacoustics of the 30P30N, but this methodology is not computationally affordable for full airplane geometries (such as the HL-CRM)

Overset Grid System: RANS

- 2D RANS Grid Refinement Study

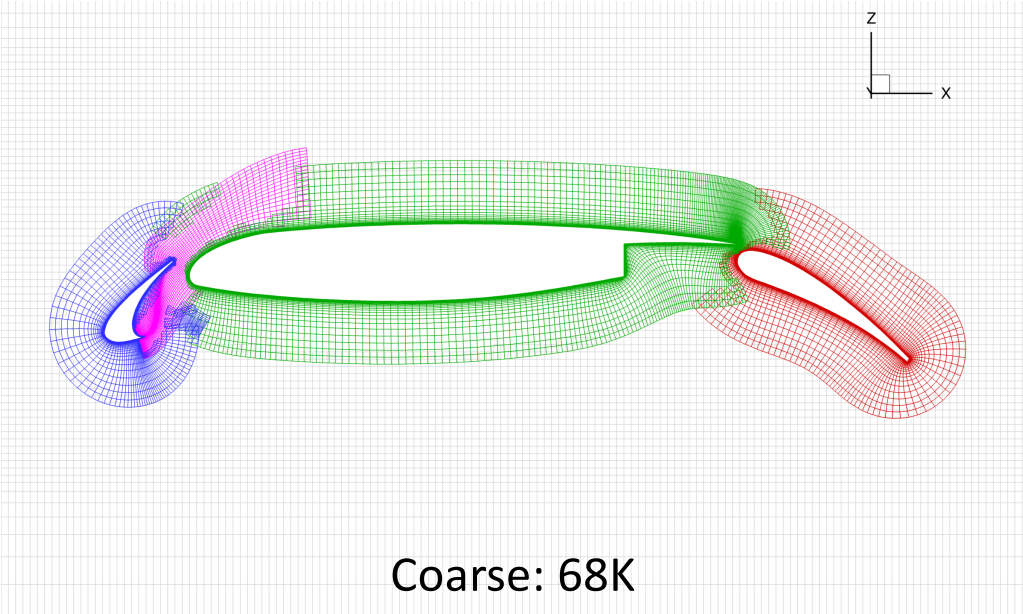

Coarse: 68K

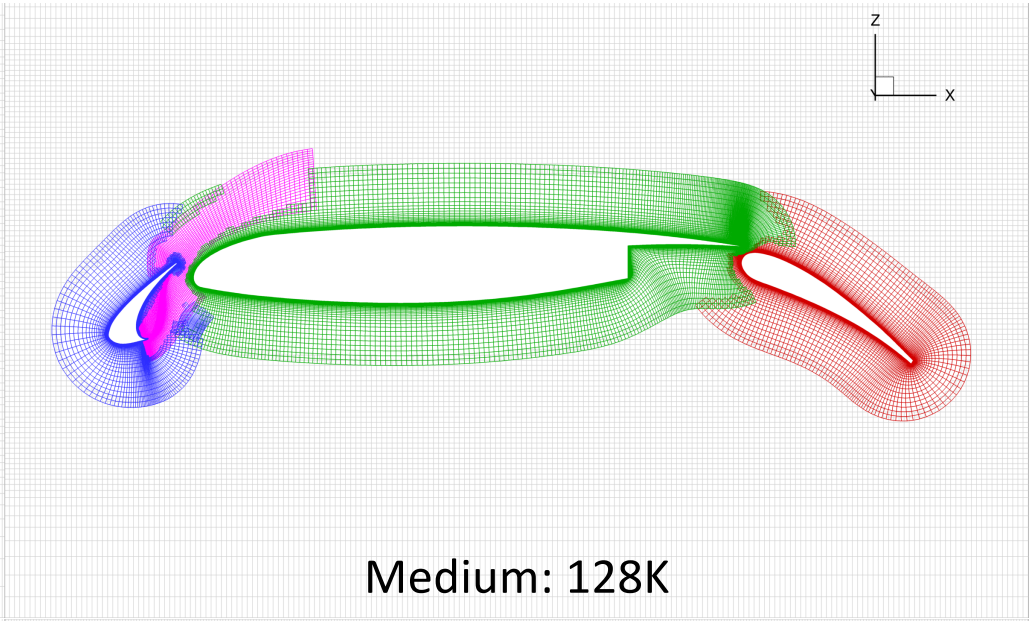

Medium: 128K

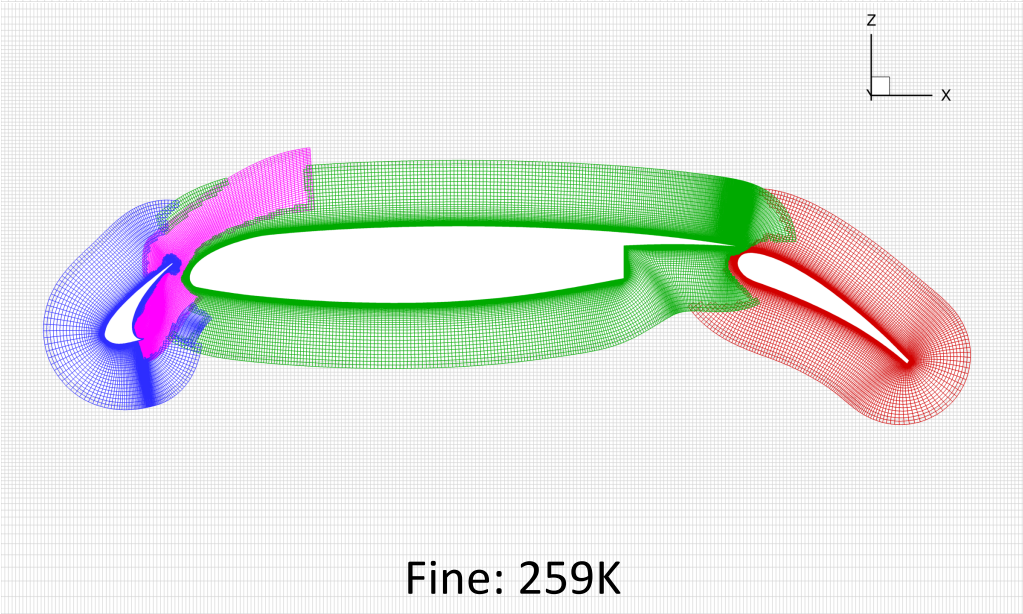

Fine: 259K

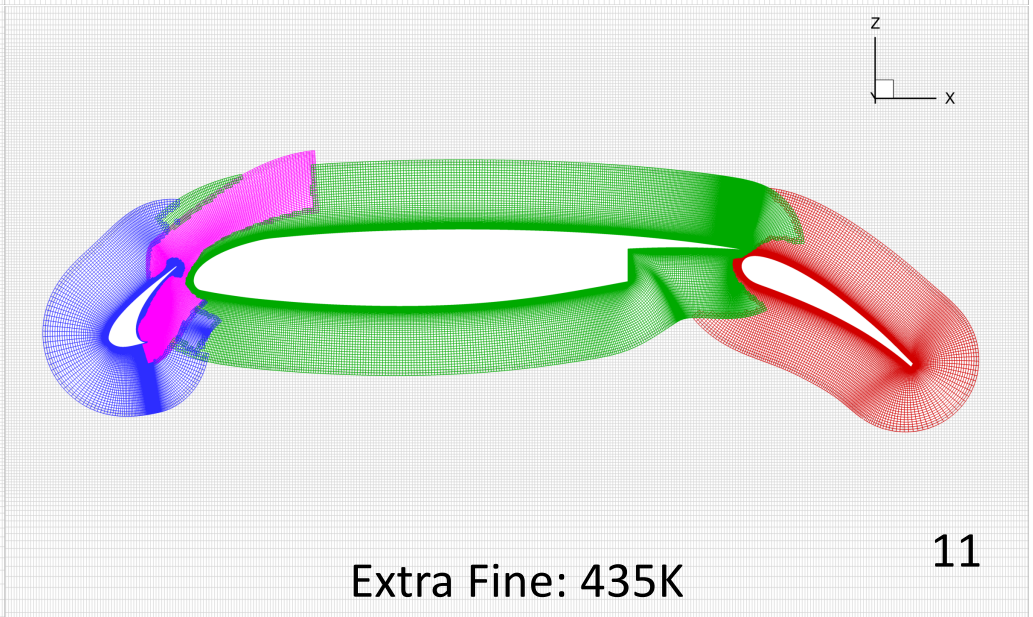

Extra Fine: 435K

Overset Grid System: RANS

- 2D RANS Grid Refinement Study

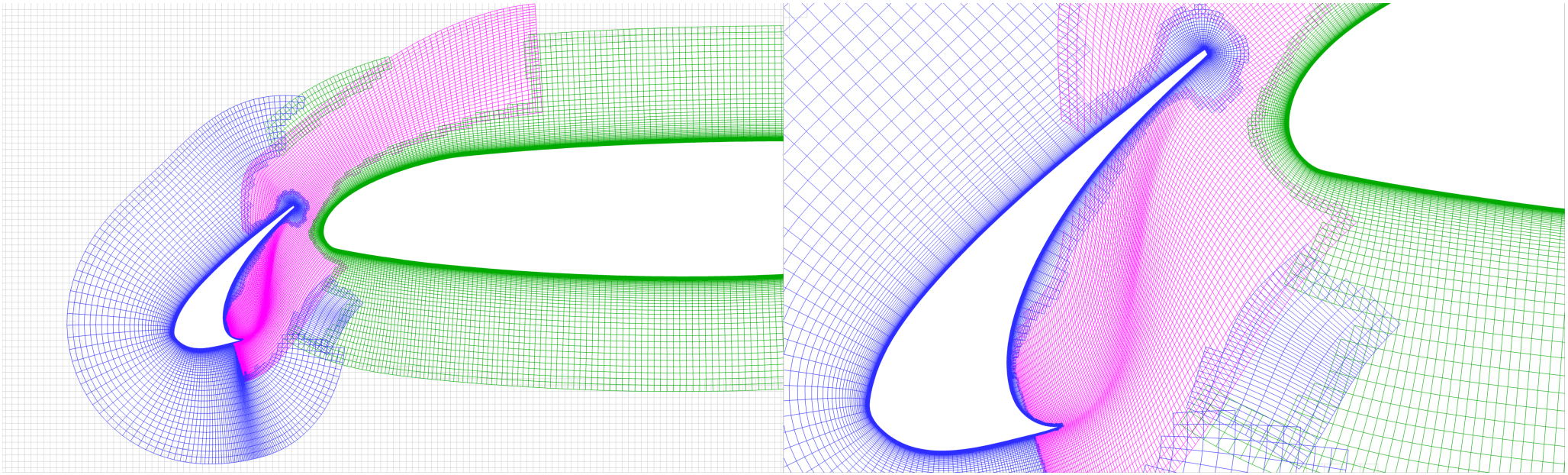

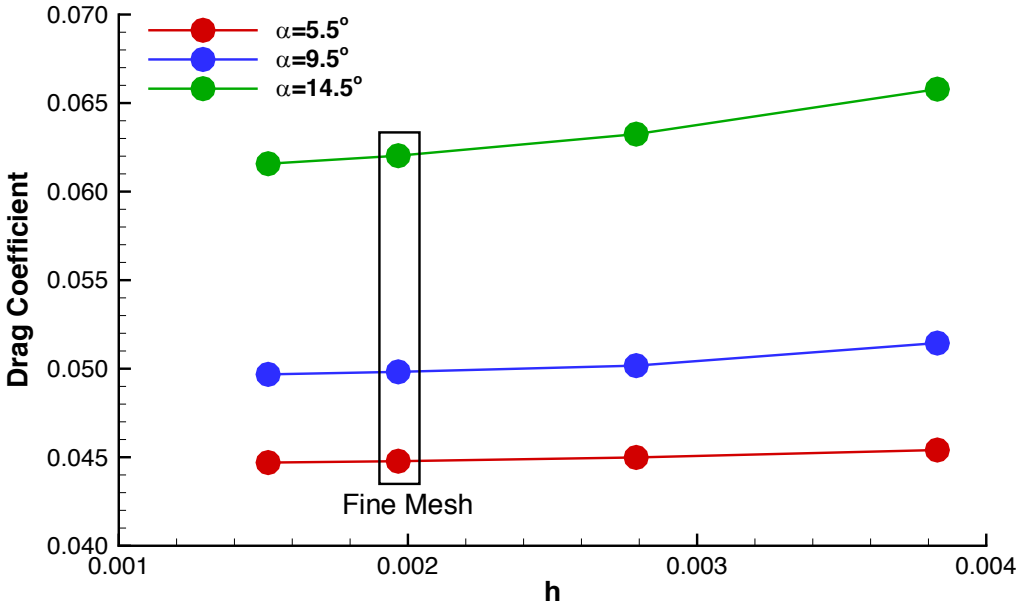

- Performed 2D steady-state RANS mesh refinement study
- Examined convergence of the lift and drag coefficient as a function of mesh spacing
- Fine grid drag coefficient is within 4 drag counts of extra fine result for each angle of attack

RANS Flow Field Visualization

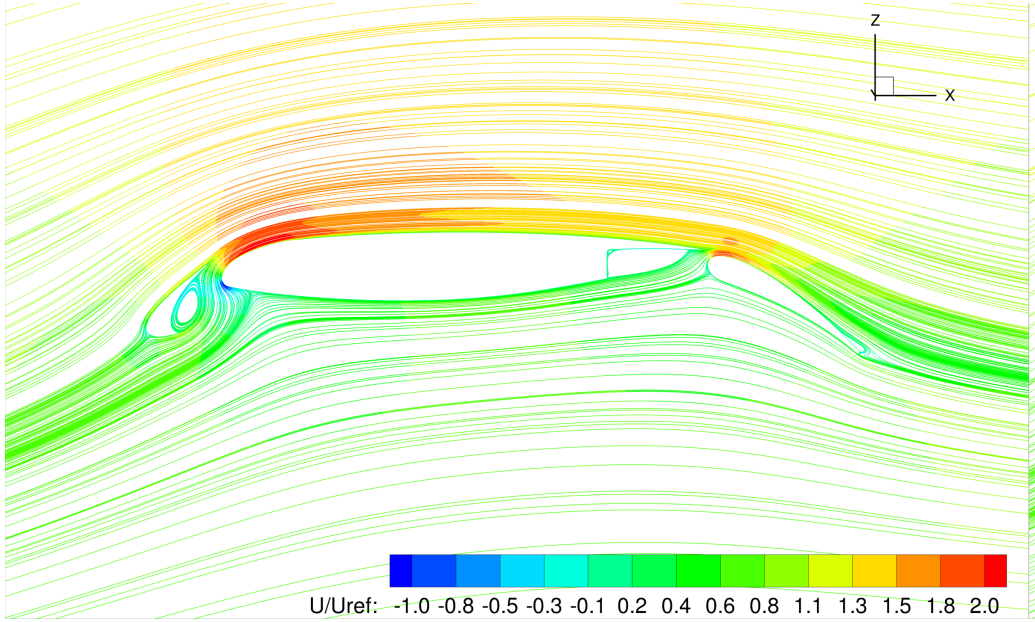

AOA = 5.5º

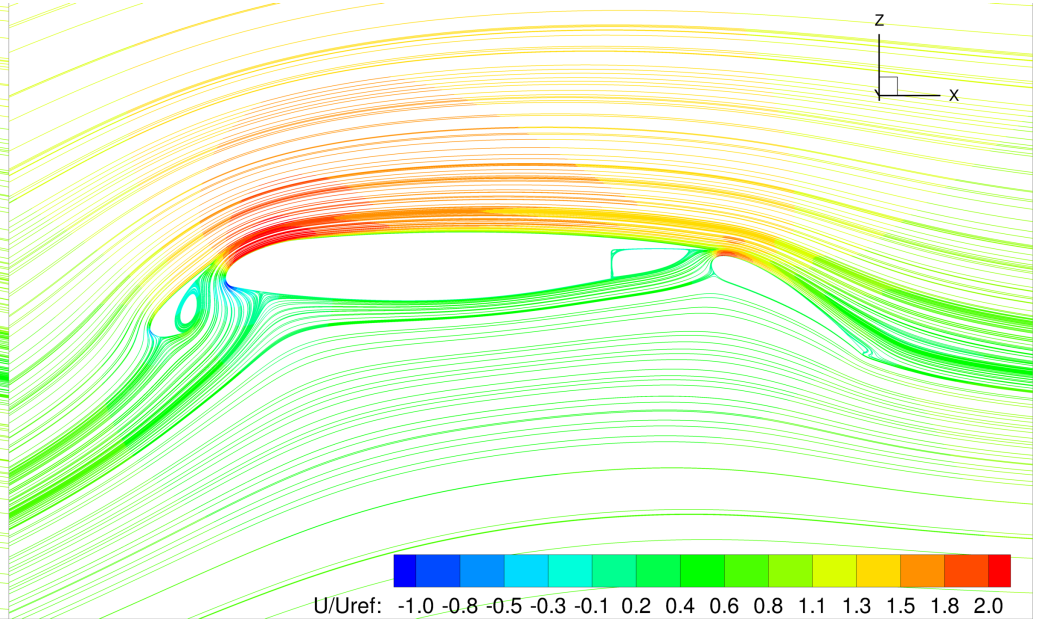

AOA = 9.5º

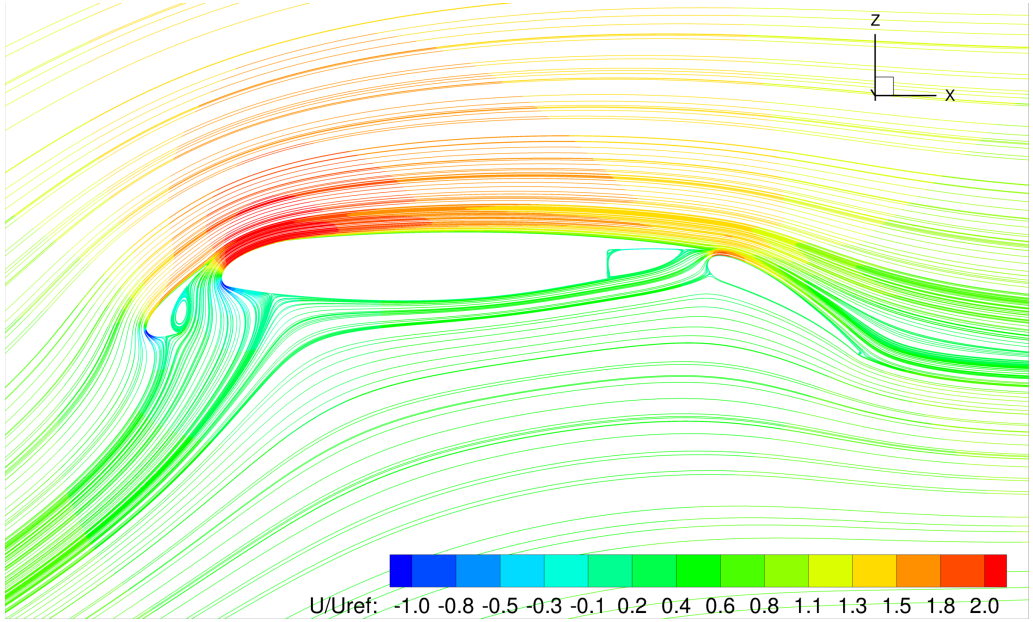

AOA = 14.5º

- RANS solution on fine mesh
- Streamlines colored by normalized velocity at AOA = 5.5, 9.5, and 14.5 degrees
- Stagnation point moves downstream with increasing AOA and slat cove wake impingement moves upstream of slat TE
- Size of elevated velocity region through the slat gap increases with AOA

Angle of Attack Shift for WT Comparison

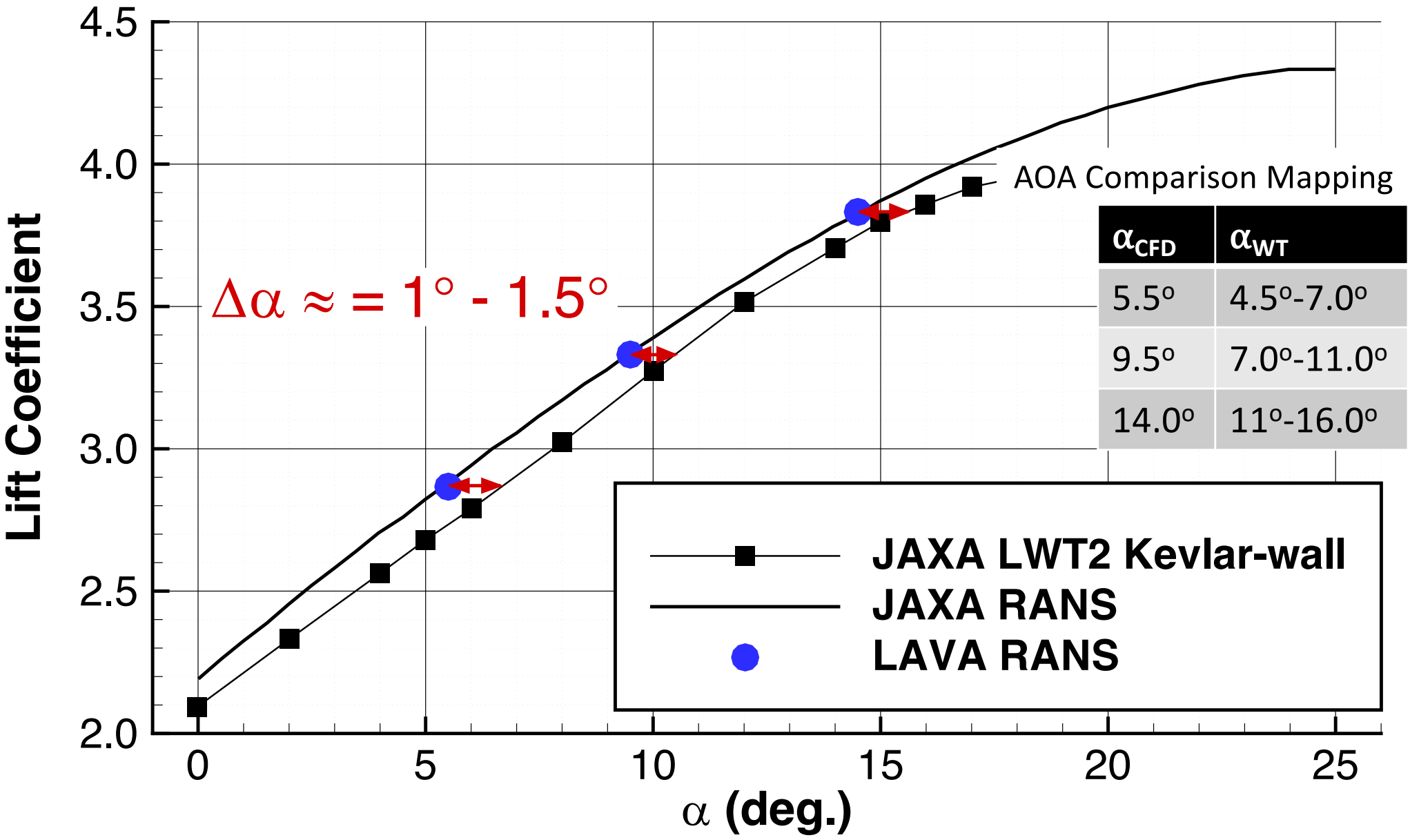

AOA Comparison Mapping

α_{CFD}	α_{WT}
5.5°	4.5°-7.0°
9.5°	7.0°-11.0°
14.0°	11°-16.0°

JAXA results from AIAA-2018-3460 *Murayama et. al.*

RANS Cp Comparison: Fine Grid

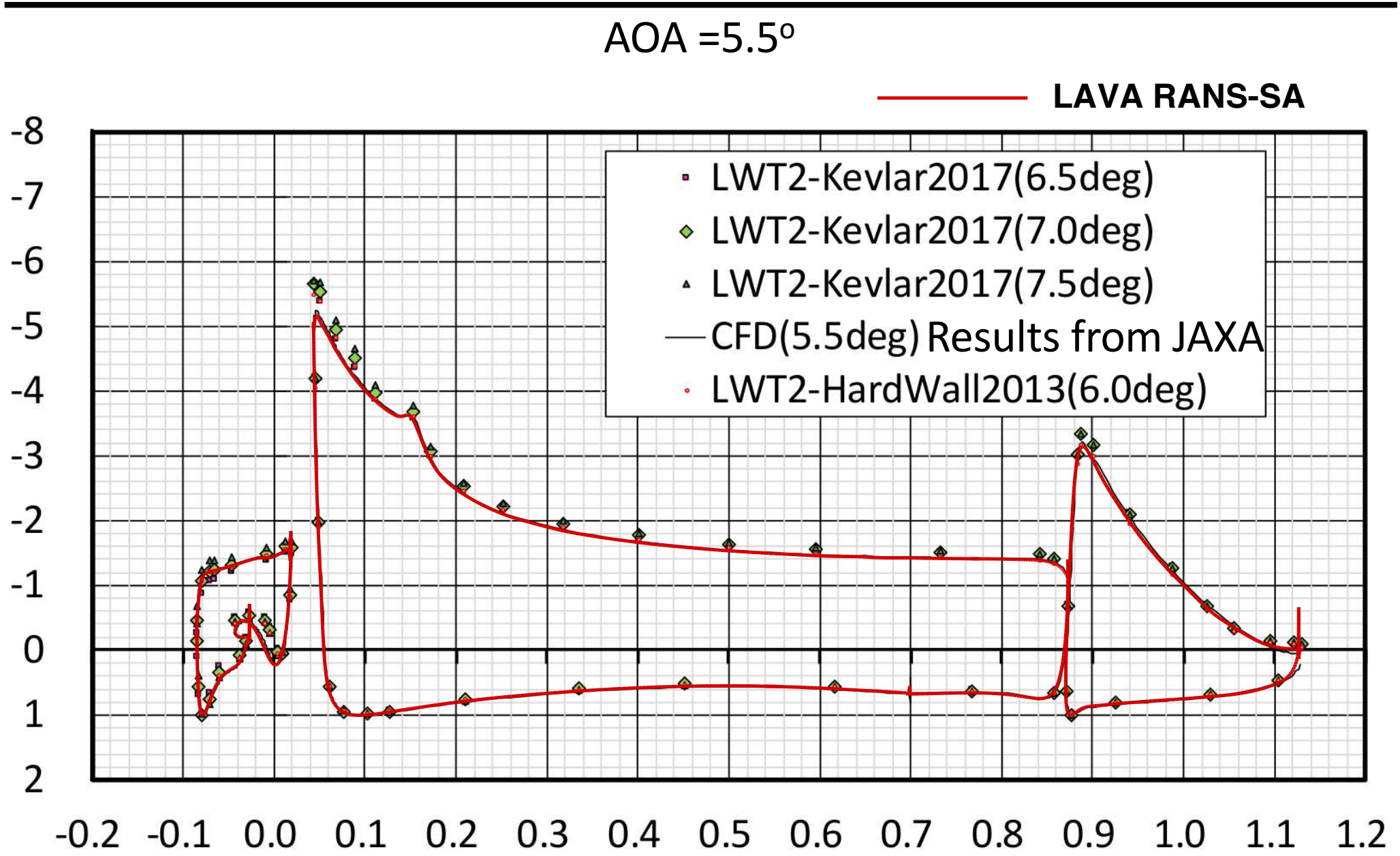

RANS Cp Comparison: Fine Grid

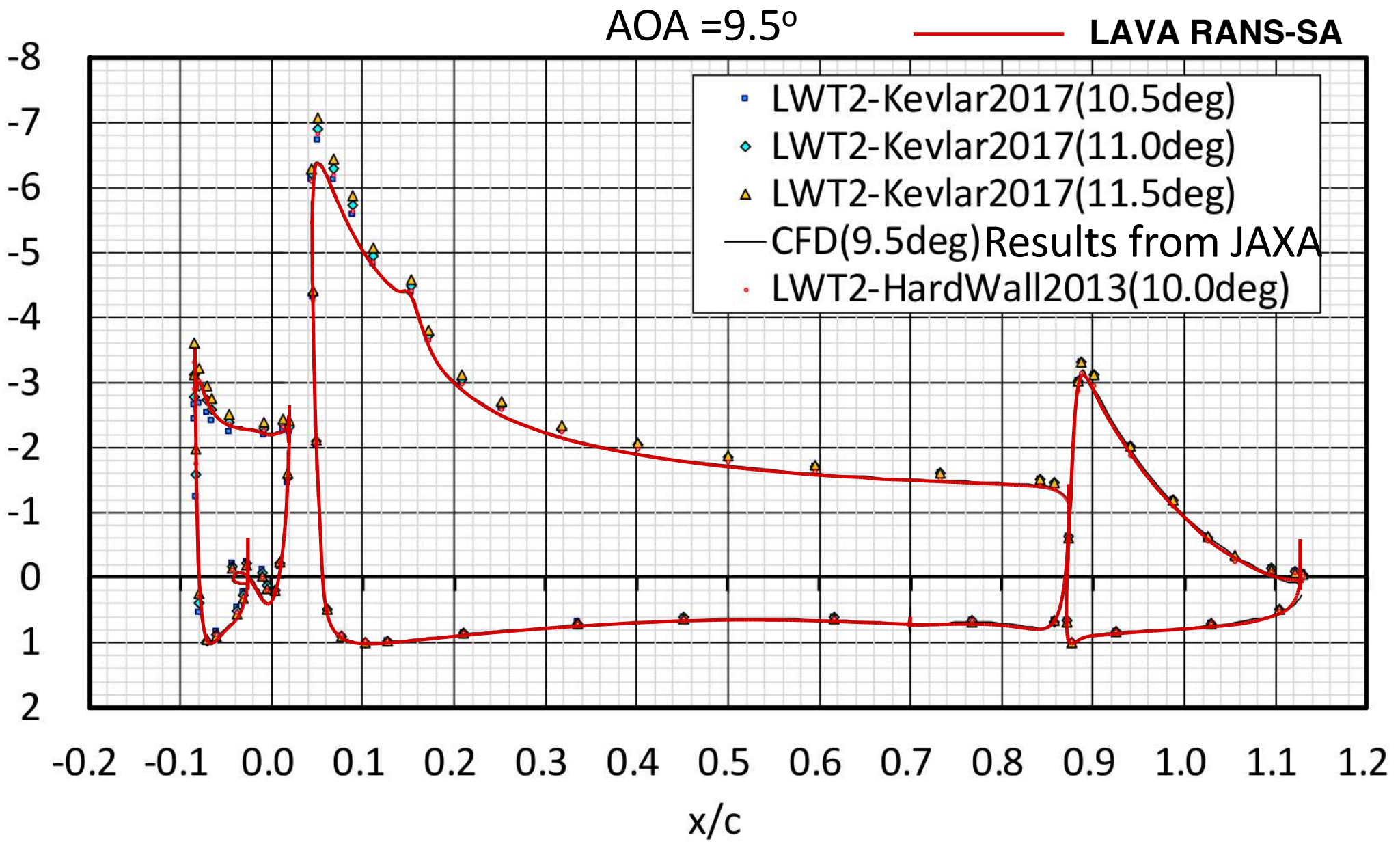

RANS Cp Comparison: Fine Grid

AOA =14.5°

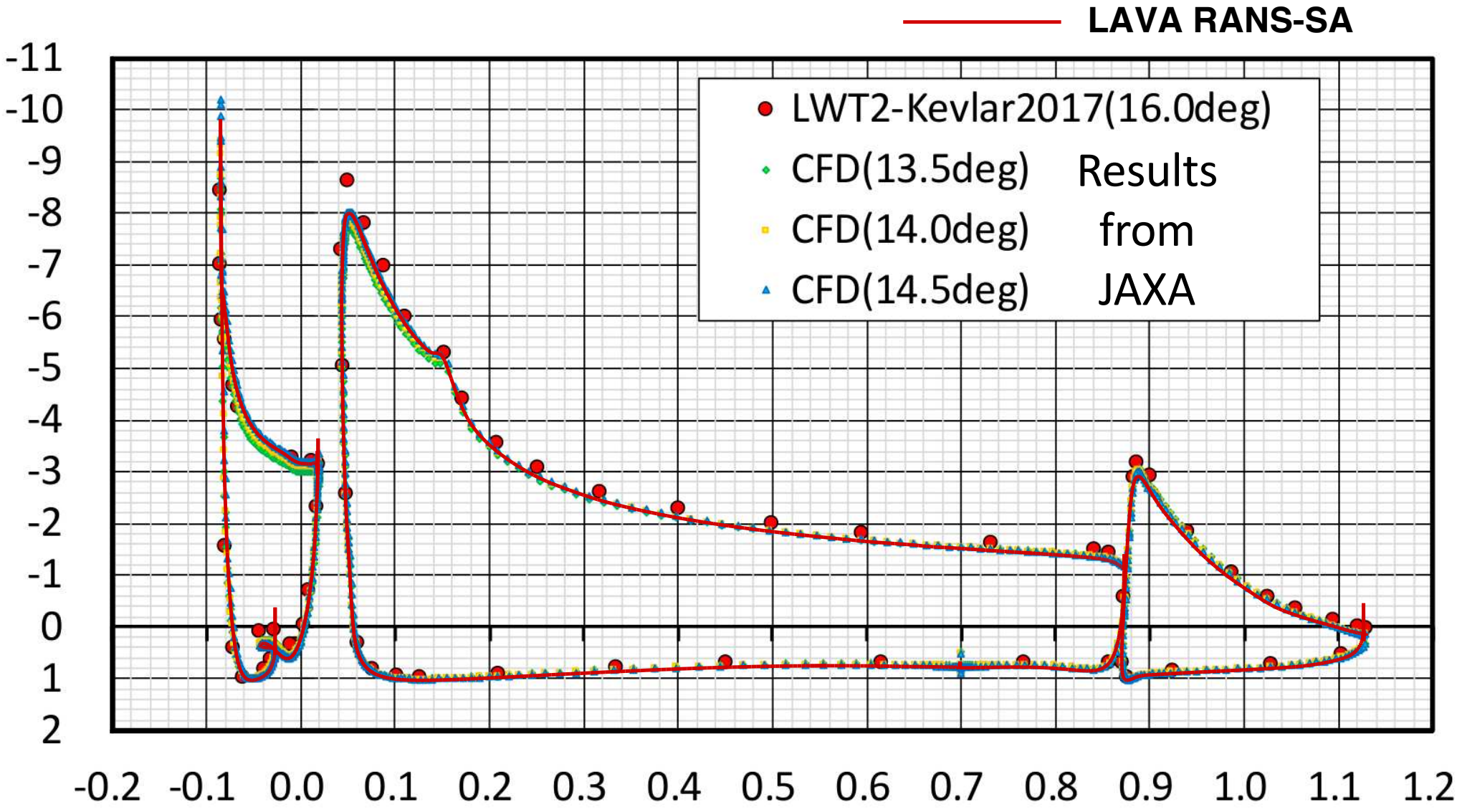

RANS Slat Cp Comparison: Fine Grid

- Excellent agreement with RANS results from JAXA are observed using the fine mesh
- Good agreement with the experiement is also observed at the shifted AOA
  (shift was determined in Murayama *et al* AVIATION 2018)
- A small discrepancy is observed on the pressure side of the slat between -0.03 < x/c < 0.01

AOA =5.5°

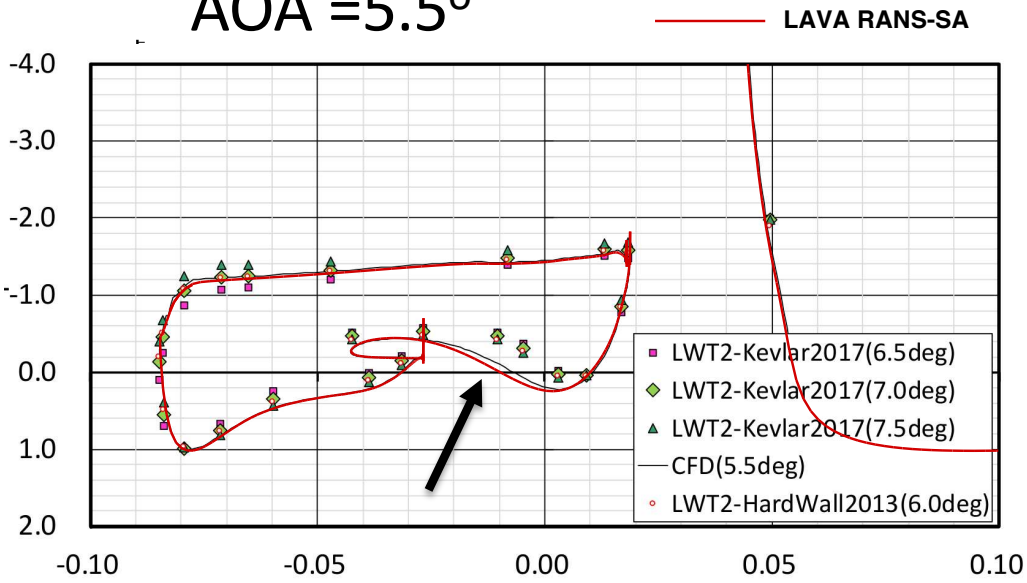

AOA =9.5°

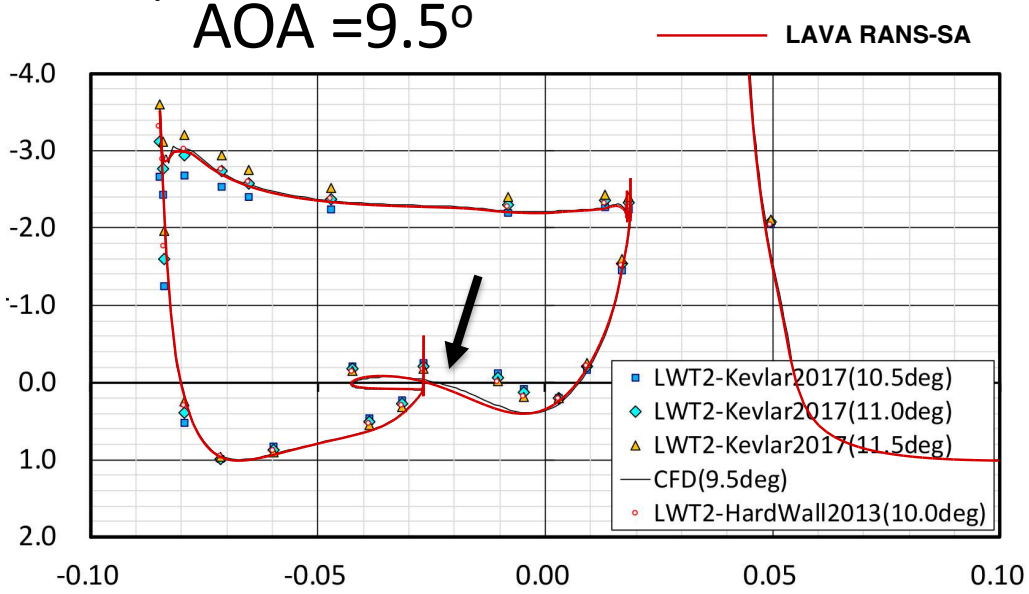

AOA =14.5°

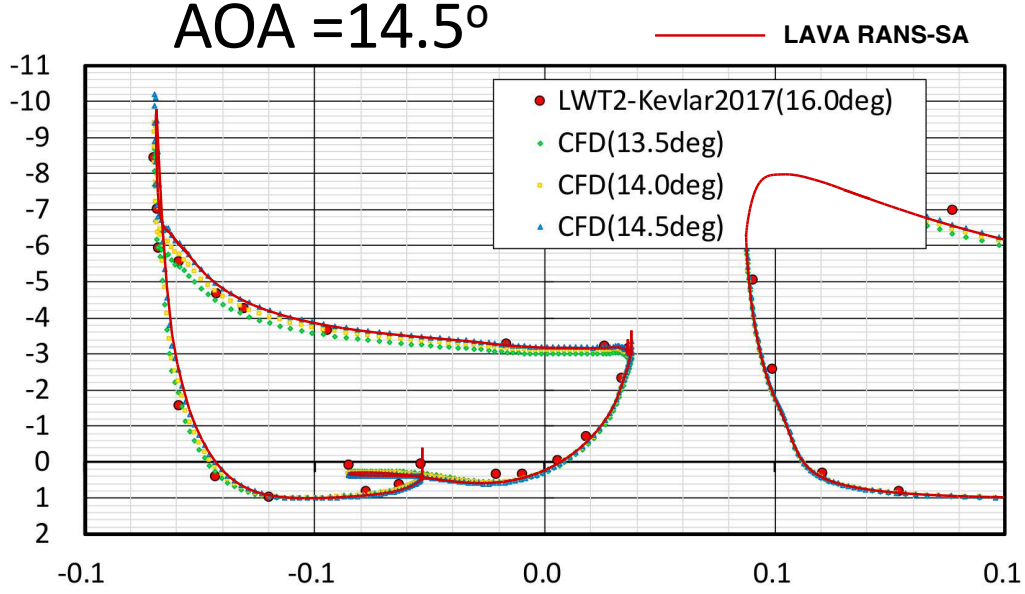

CFD Results from JAXA

Overset Grid System: ZDES

Affordable gridding approach to hybrid RANS-LES

- Spatially varying spanwise grid spacing
  - Use finest spanwise grid spacing for the slat and slat cove (red)
  - Coarsen spanwise spacing by a factor of 2 on main element and flap to capture the slat wake (green)
  - Coarsen the off-body grid by an additional factor of 2 in spanwise spacing to further reduce the computational cost (blue)

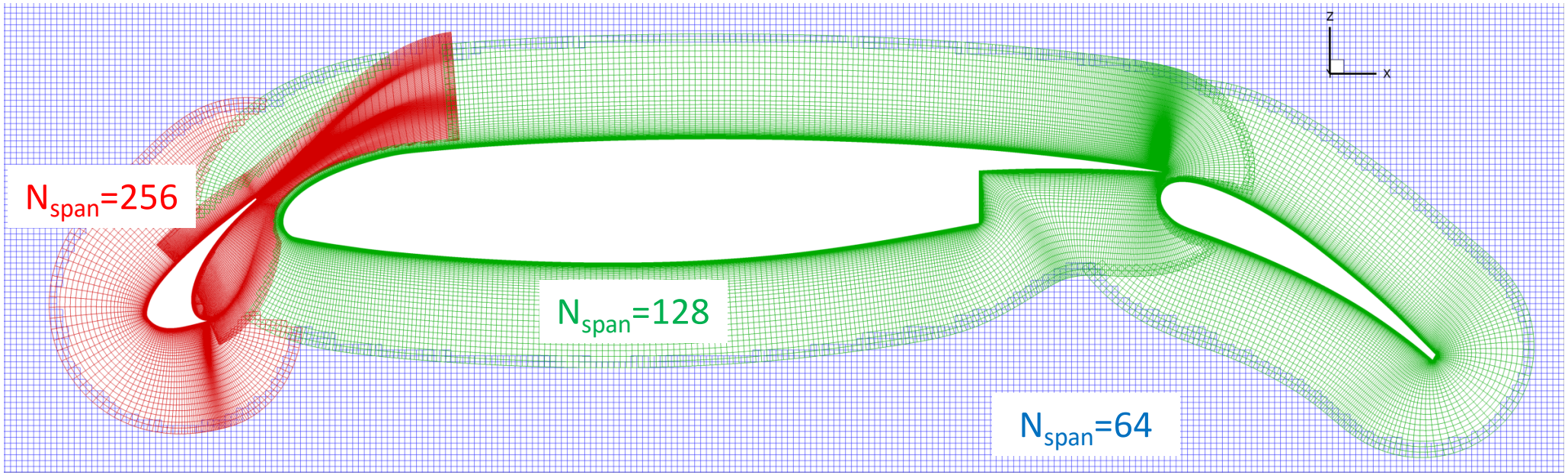

Total number of grid points: 36.7 million

Overset Grid System: ZDES

Affordable gridding approach to hybrid RANS-LES

- Zonal approach to turbulence mode

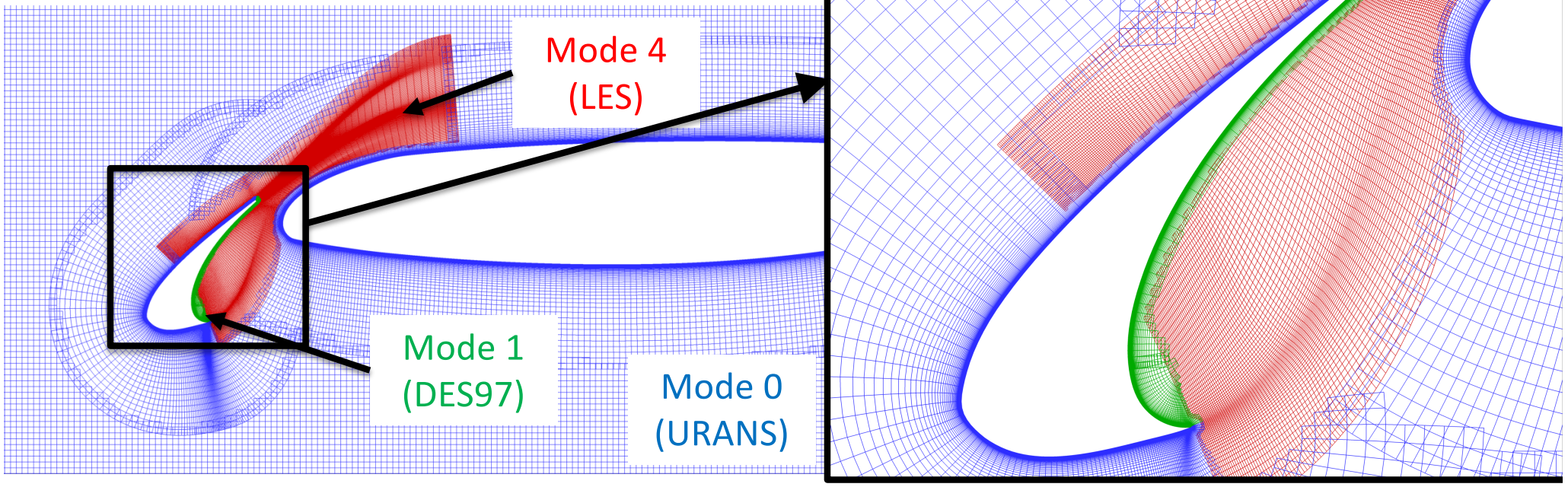

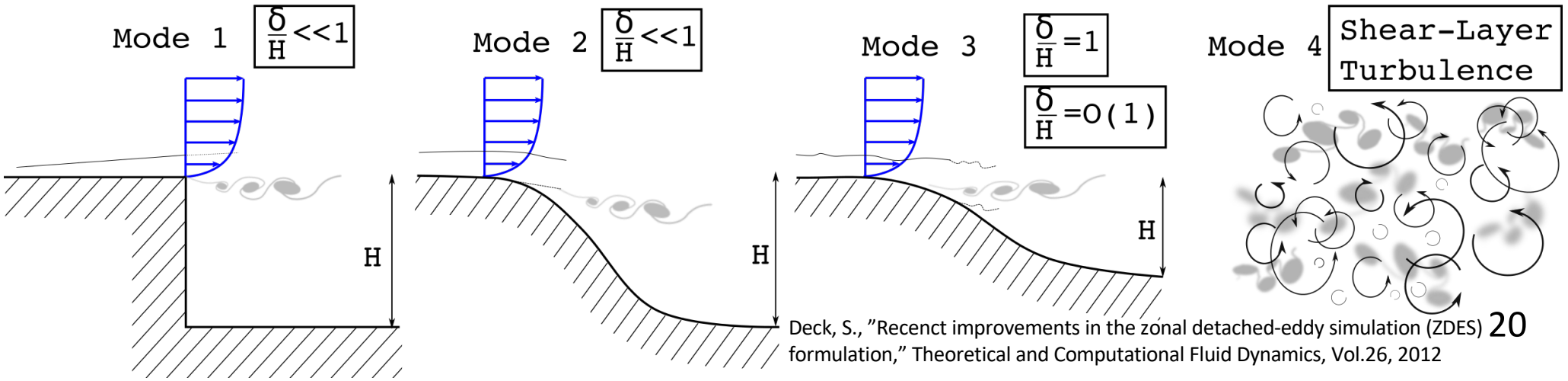

Deck, S., "Recenct improvements in the zonal detached-eddy simulation (ZDES) formulation," Theoretical and Computational Fluid Dynamics, Vol.26, 2012

Flow-Field Visualization

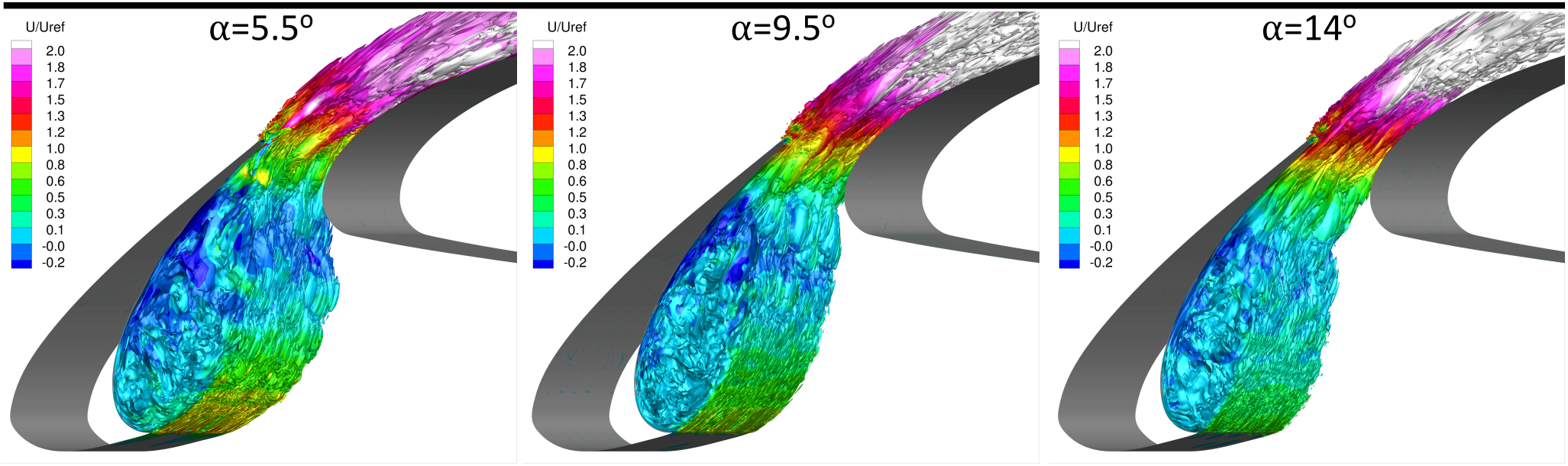

Isocontour of instantaneous x-vorticity colored by normalized velocity

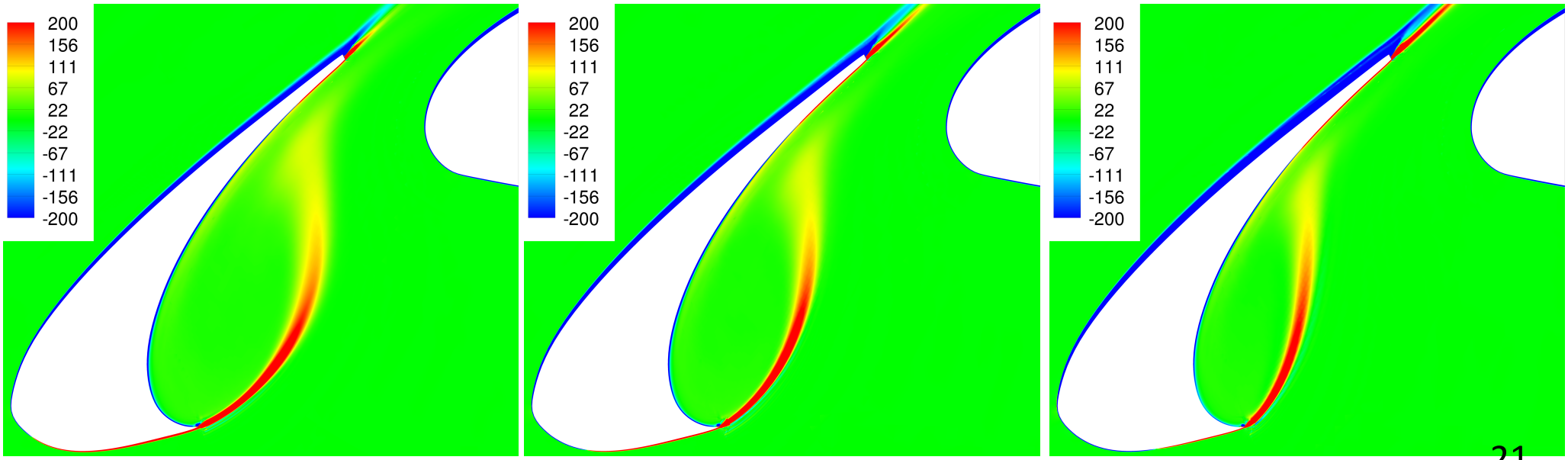

Time-averaged spanwise vorticity contours

Flow-Field Visualization

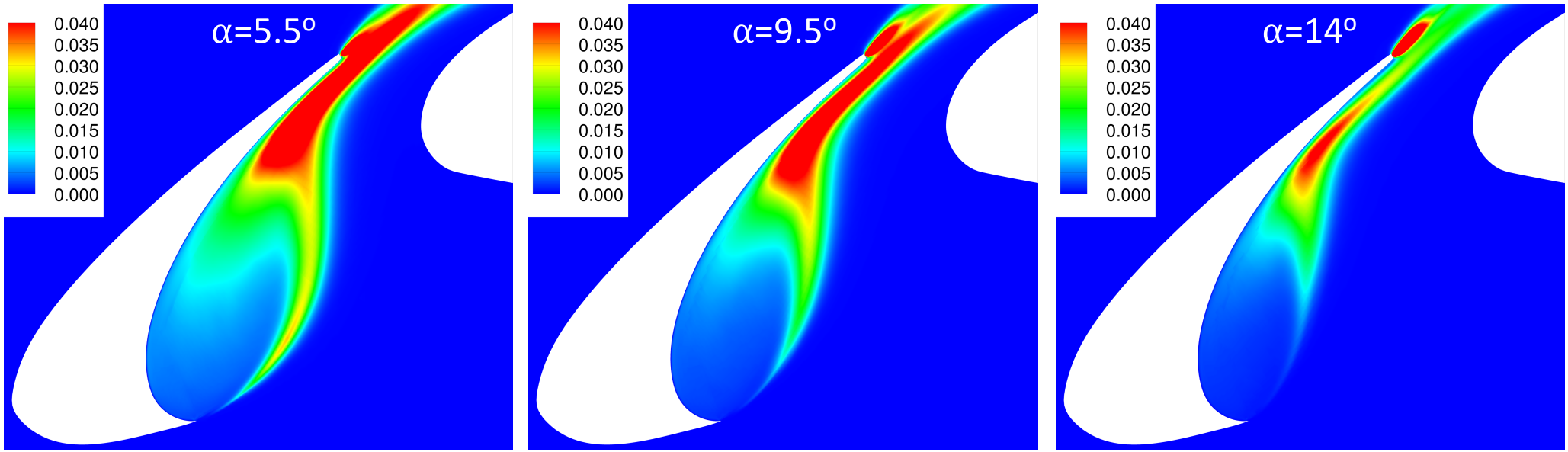

Resolved 2D turbulent kinetic energy

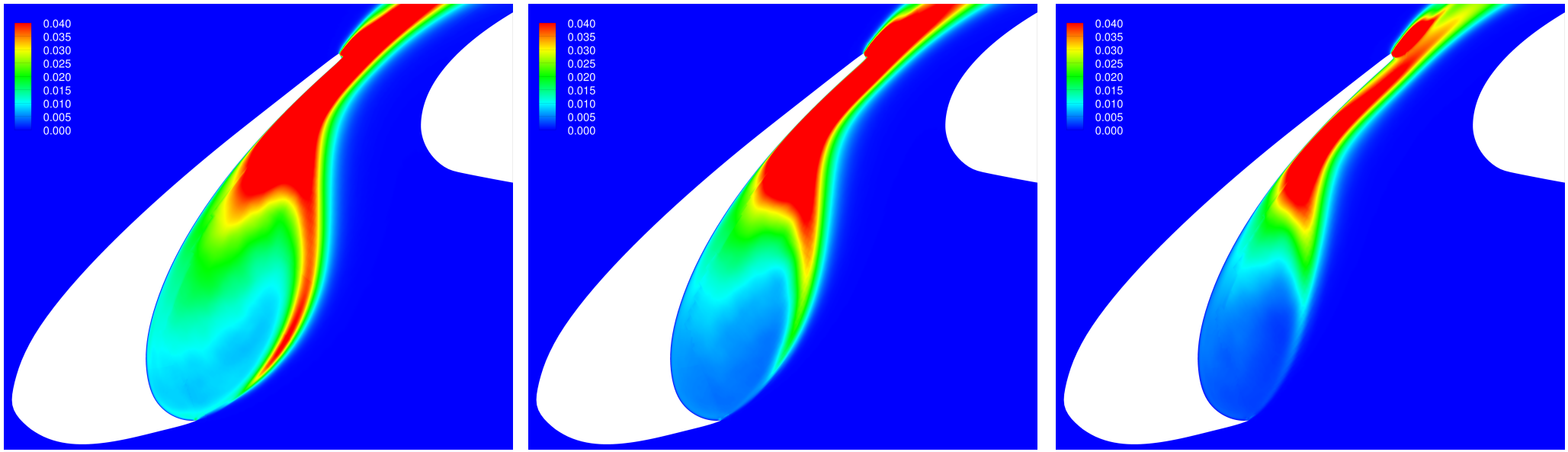

Resolved 3D turbulent kinetic energy

Flow-Field Visualization

Contour plot of instantaneous density gradient magnitude

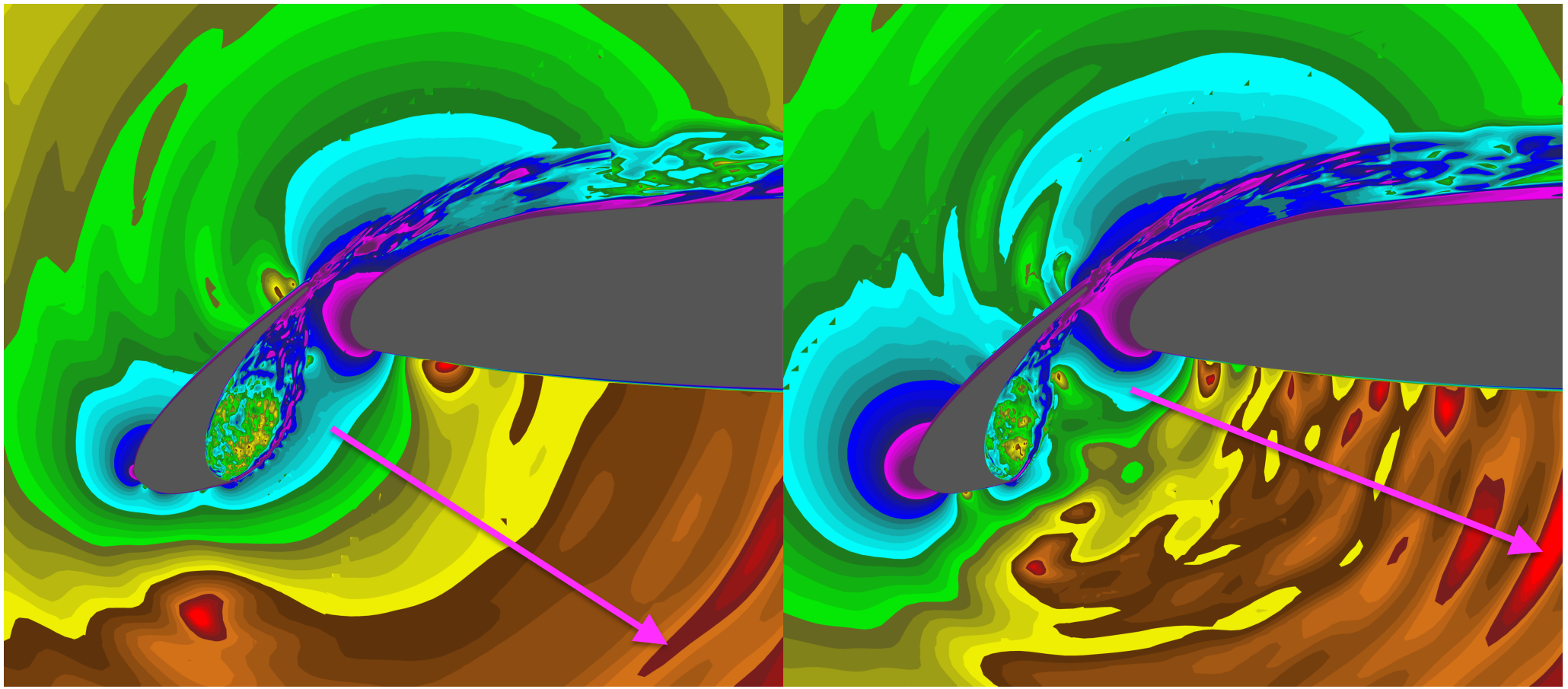

α=5.5° α=14°

- An increase in the directivity angle of the acoustic waves emanating from the slat cove are observed with increasing AOA in this vehicle fixed reference frame
- Details of the directivity dependence on AOA will be examined in the far-field section

Comparison to BANC-IV Contribution

BANC-IV Overset Grid System for hybrid RANS-LES

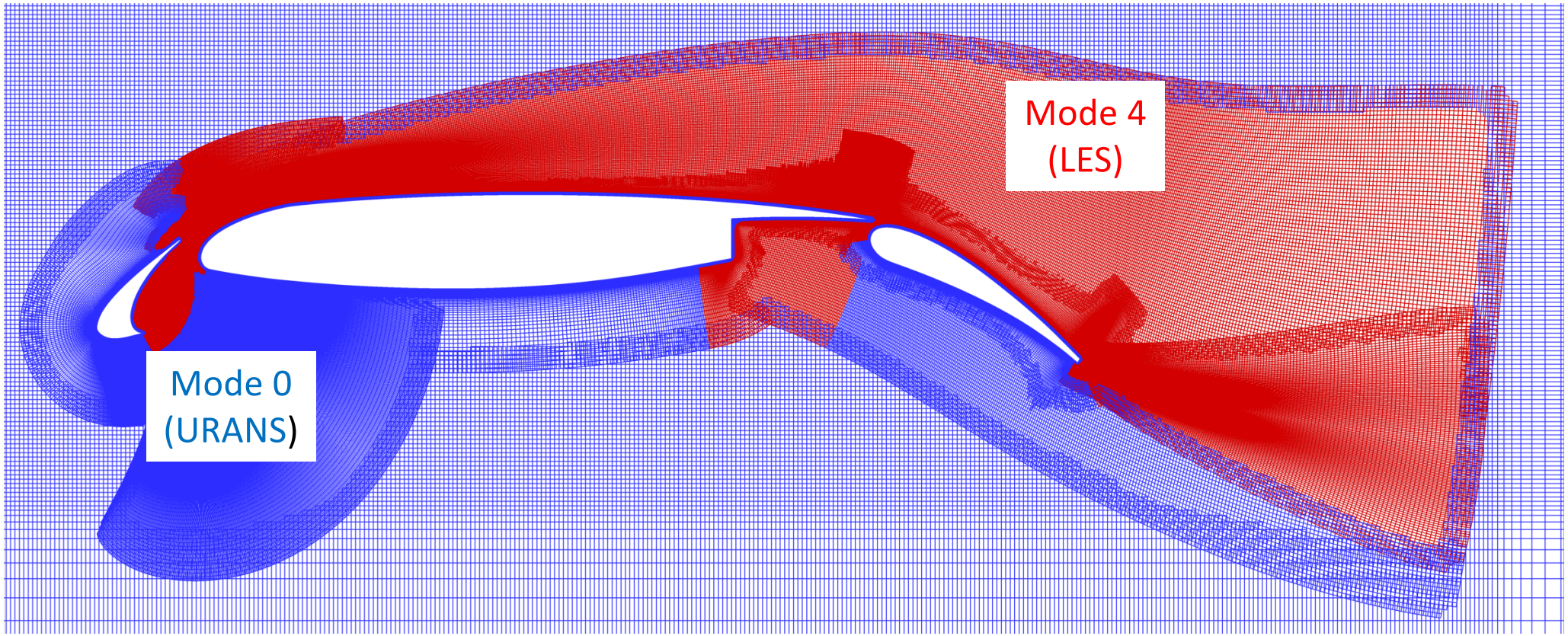

- Number of Grid Points: 78.1 M (more than double of current grid)
- Spanwise: 194 (constant throughout the mesh include Mode 0)
- 6^{th} order HWCNS with blended $6^{th}/5^{th}$ central/upwind state interpolation (requires triple fringe points as opposed to double)
- 8^{th} order HWCNS with blended $8^{th}/7^{th}$ interpolation used in span

Flow-Field Visualization

BANC-IV Contribution (α=5.5º)

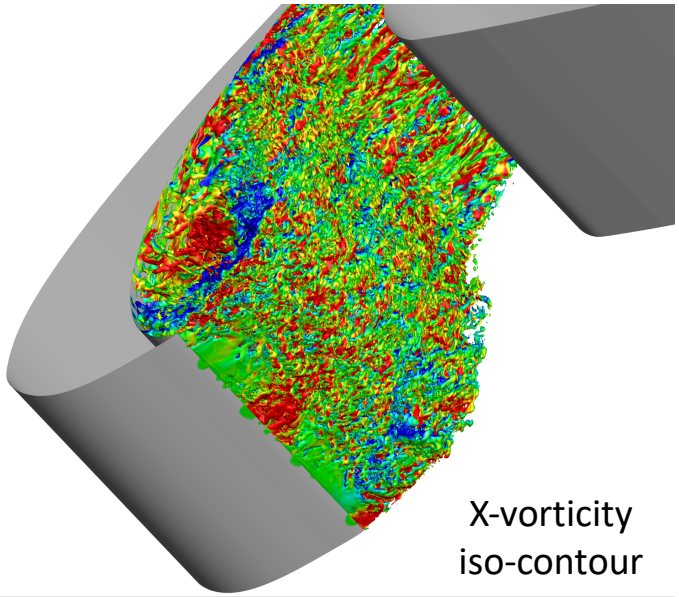

X-vorticity
iso-contour

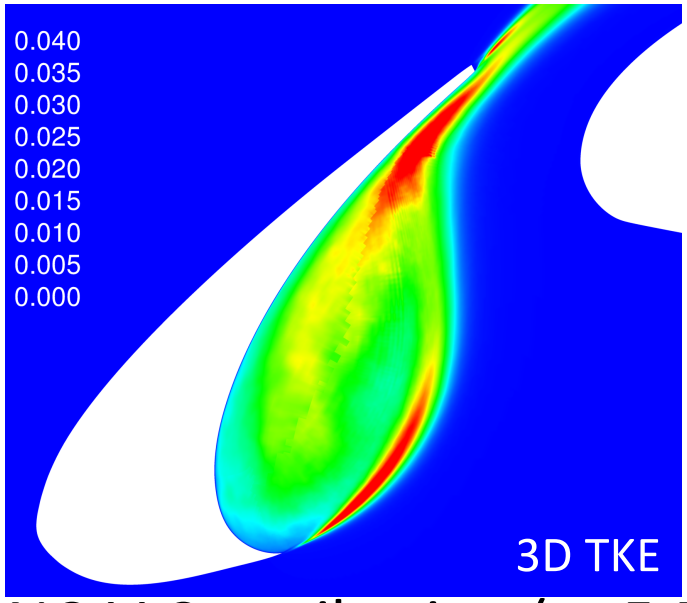

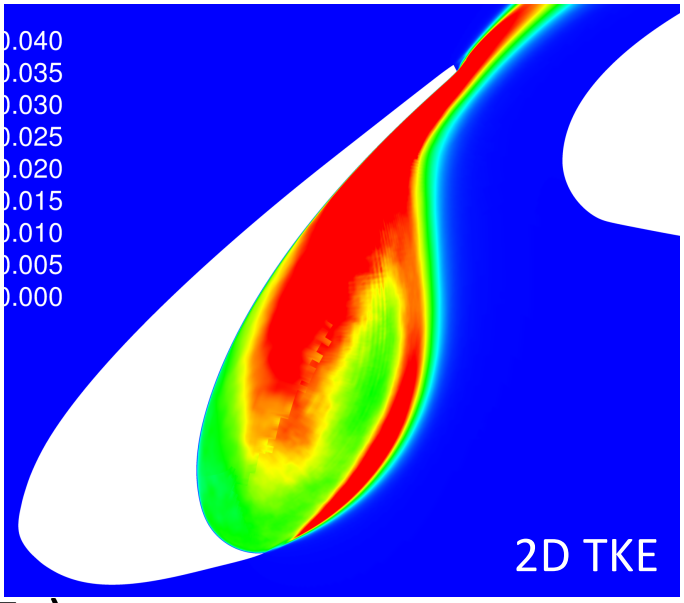

BANC-V Contribution (α=5.5º)

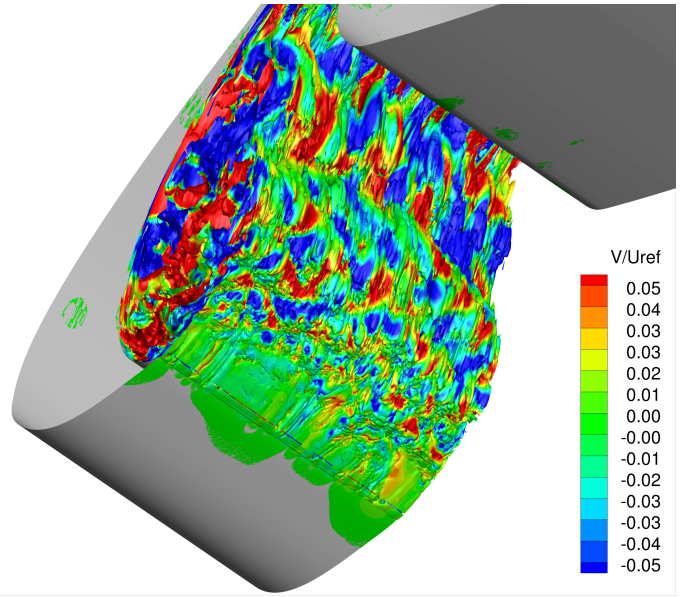

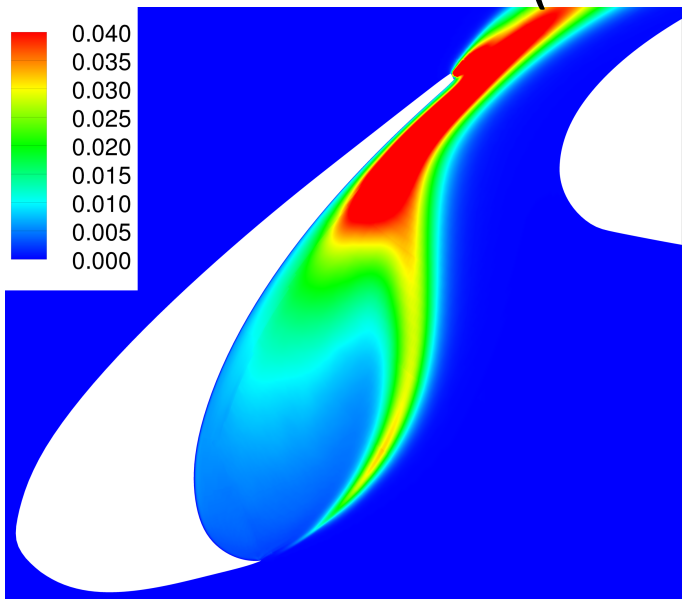

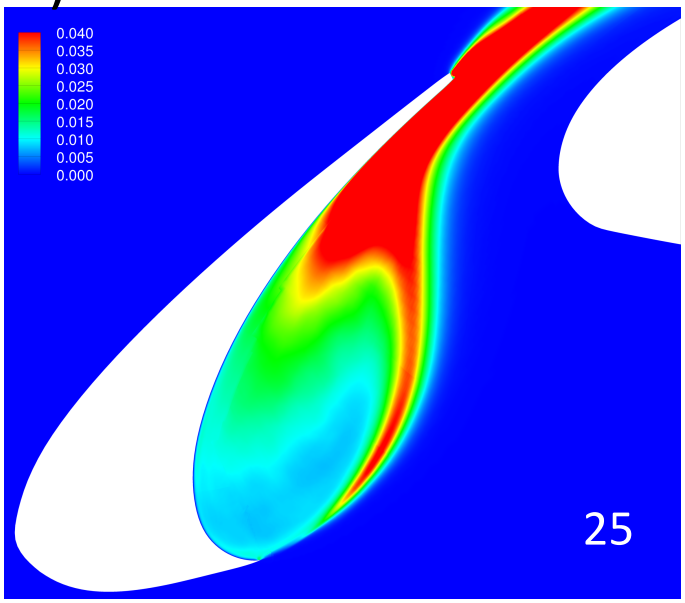

PSD Sensor Diagram

- Power Spectral Density (PSD) of pressure was recorded at 10 sensor locations
- Locations 1 and 9 are positioned on the LE of the main element
- Locations 2-5 are inside the slat cove
- Locations 6-8 are on the exterior of the slat
- Location 10 is on the flap

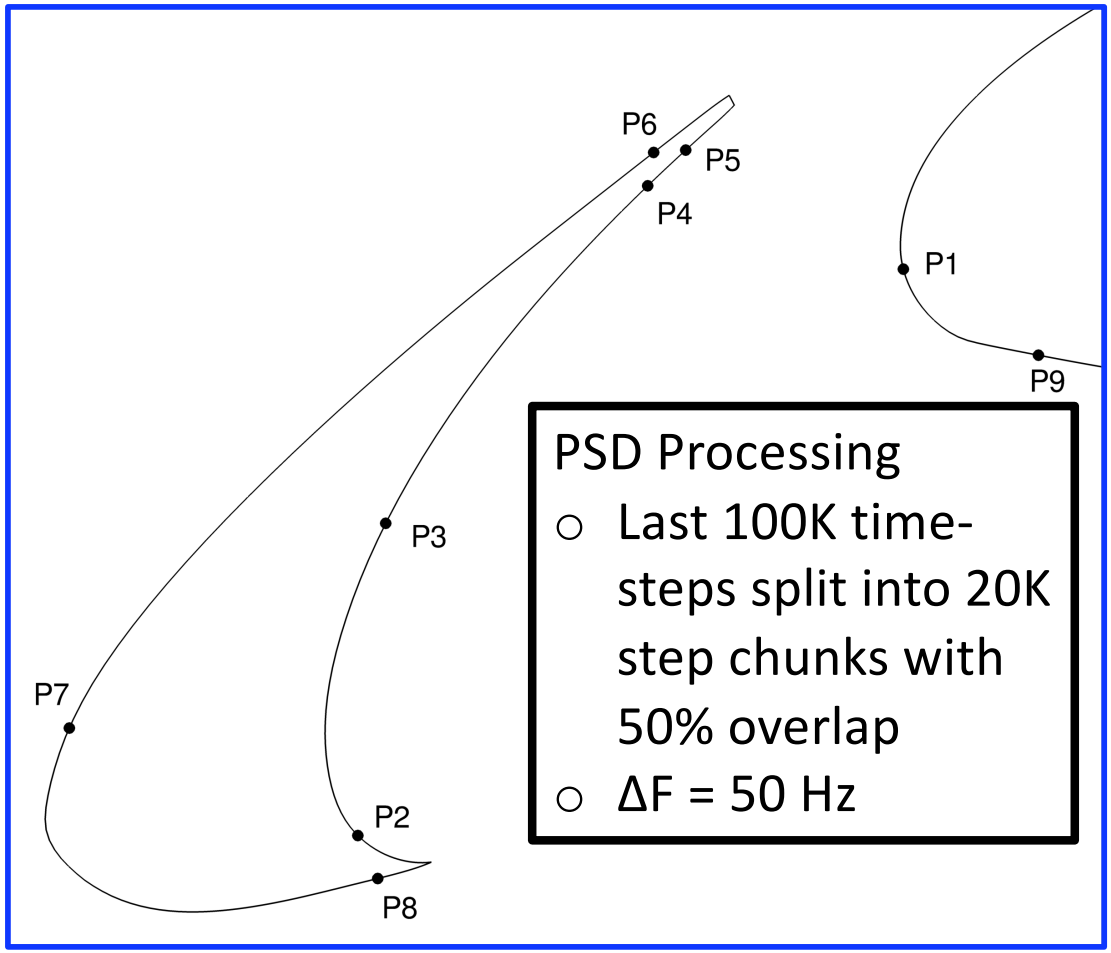

PSD Processing
- Last 100K time-steps split into 20K step chunks with 50% overlap
- ΔF = 50 Hz

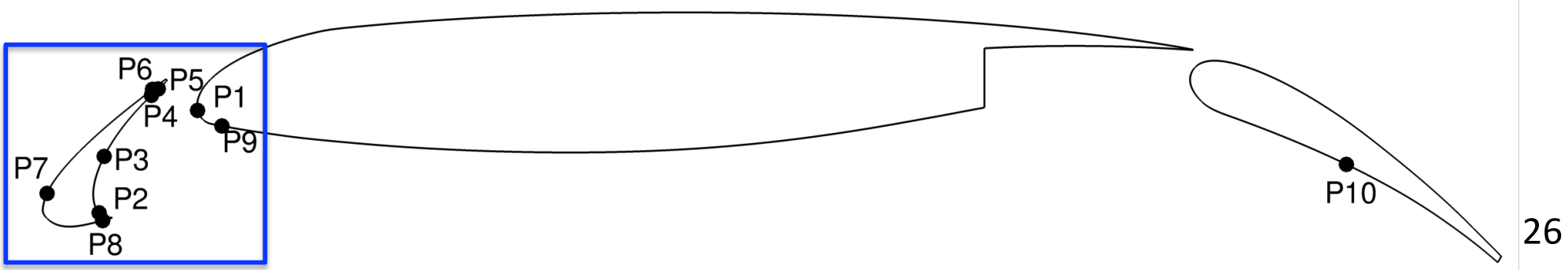

Comparison to Previous BANC Results

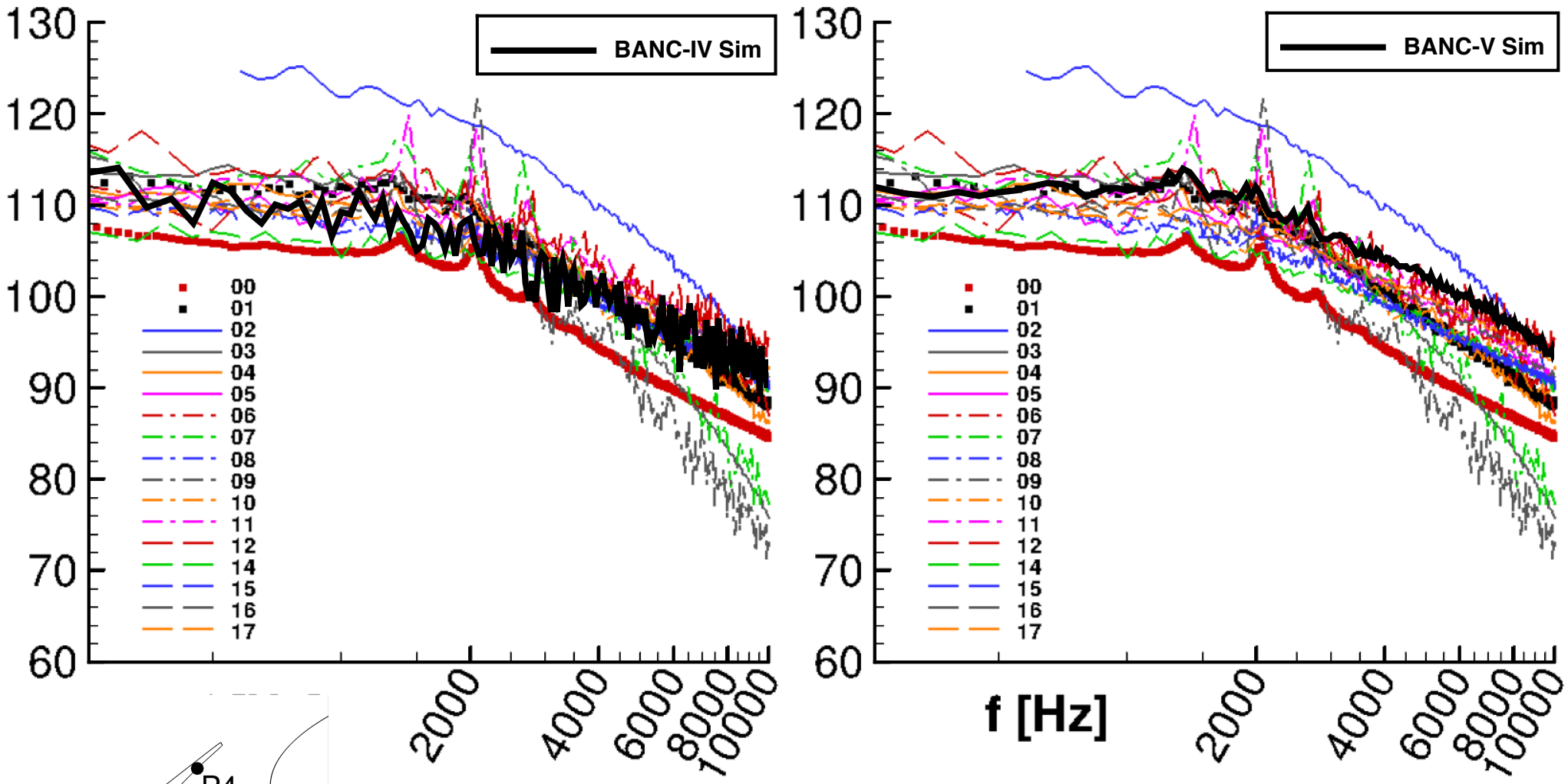

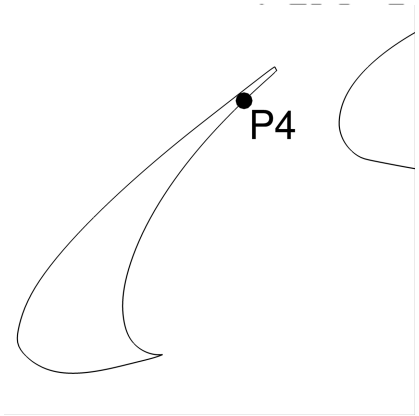

- Slightly higher PSD levels are observed in the BANC-V Sim compared to BANC-IV and fall on top of 01 (JAXA LWT2 Hard Wall WT Data) for frequencies below 3 kHz

Comparison to Previous BANC Results

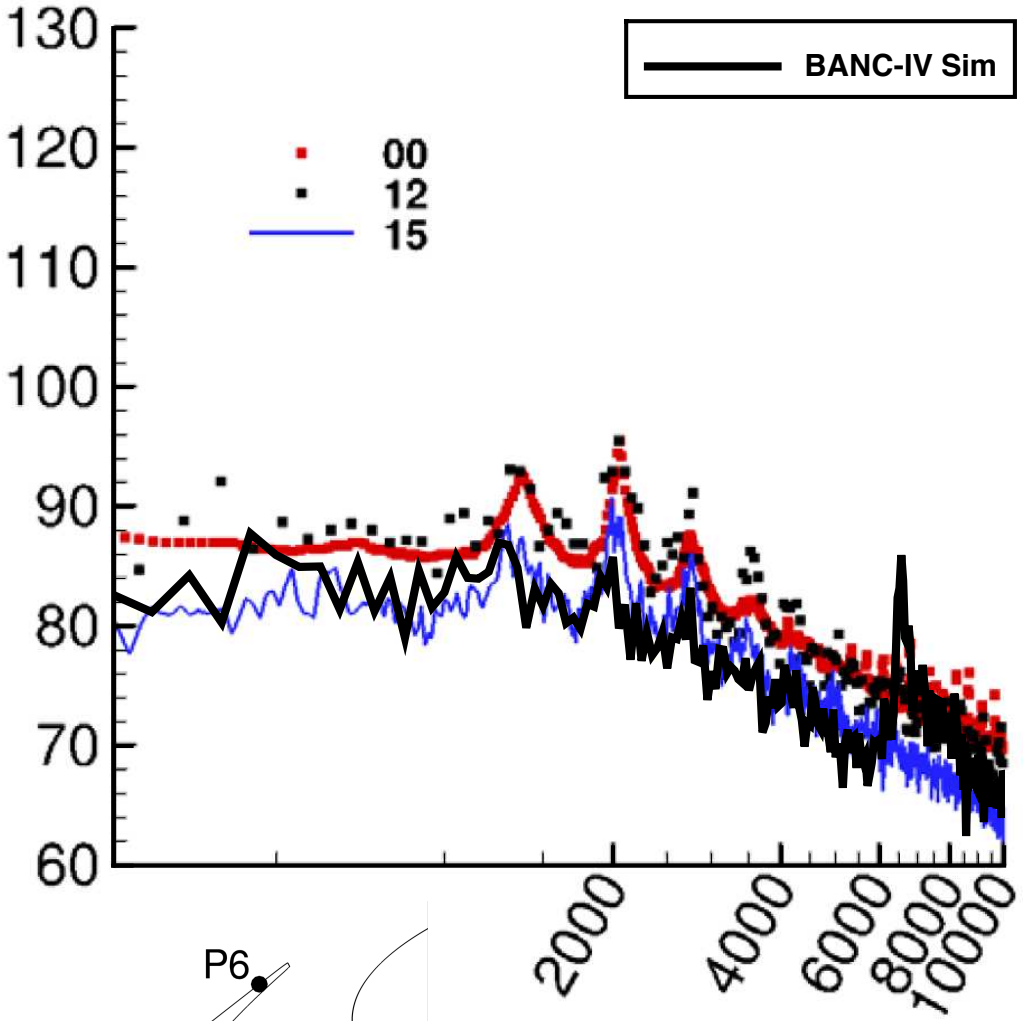

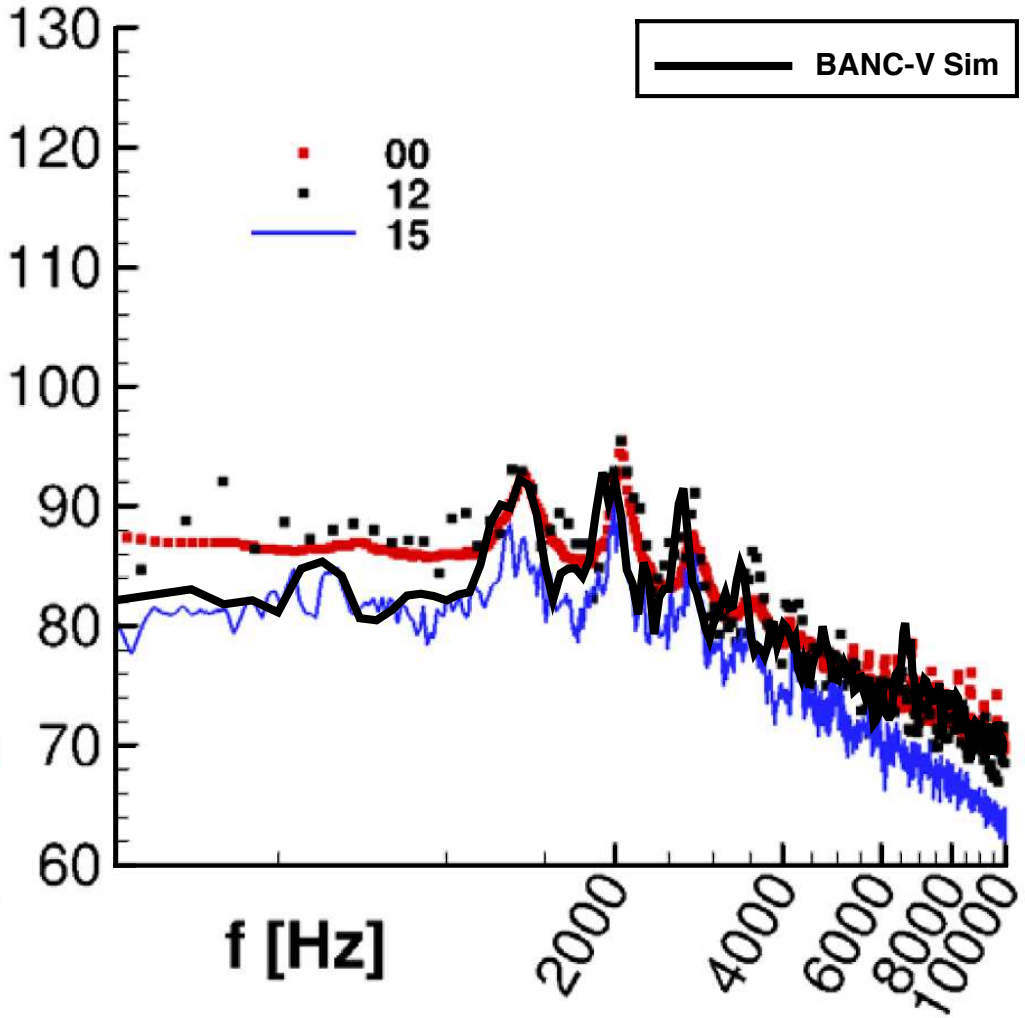

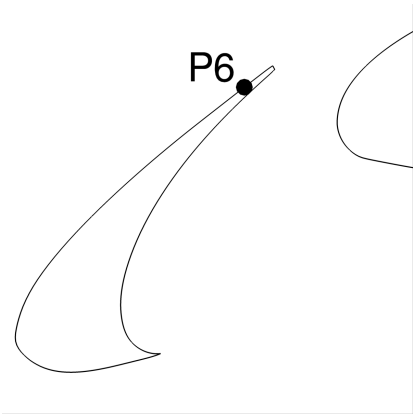

Larger narrow band peaks observed in BANC-V Sim which match both the amplitude and frequencies observed in 00 (FSU WT) and 01 (JAXA LWT2 Hard Wall WT) Data

Near-Field Results

PSD at sensor location 4

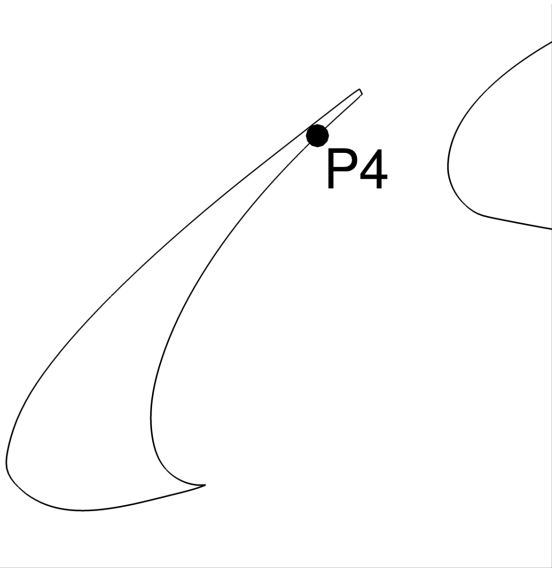

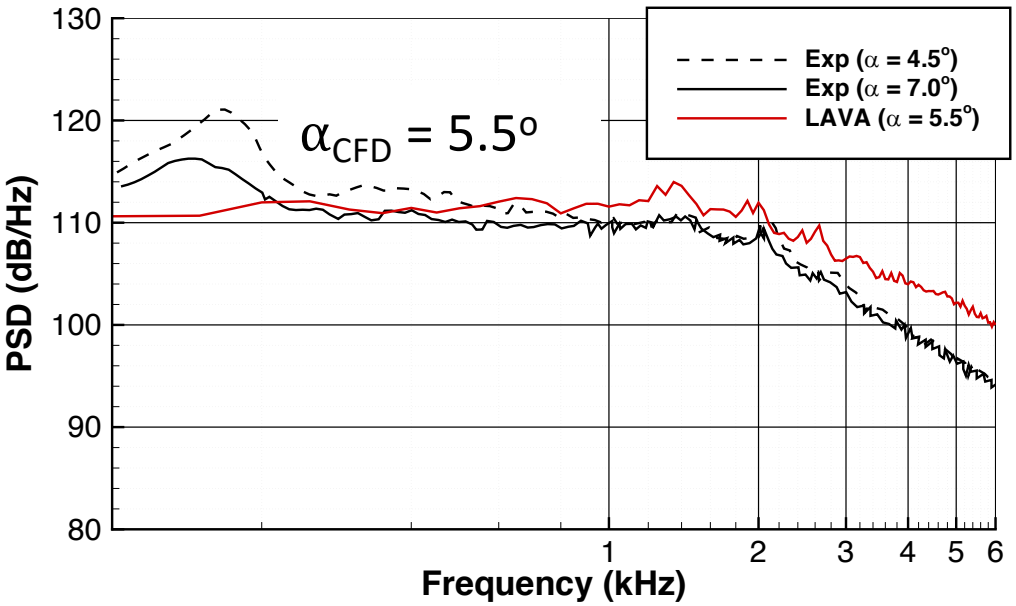

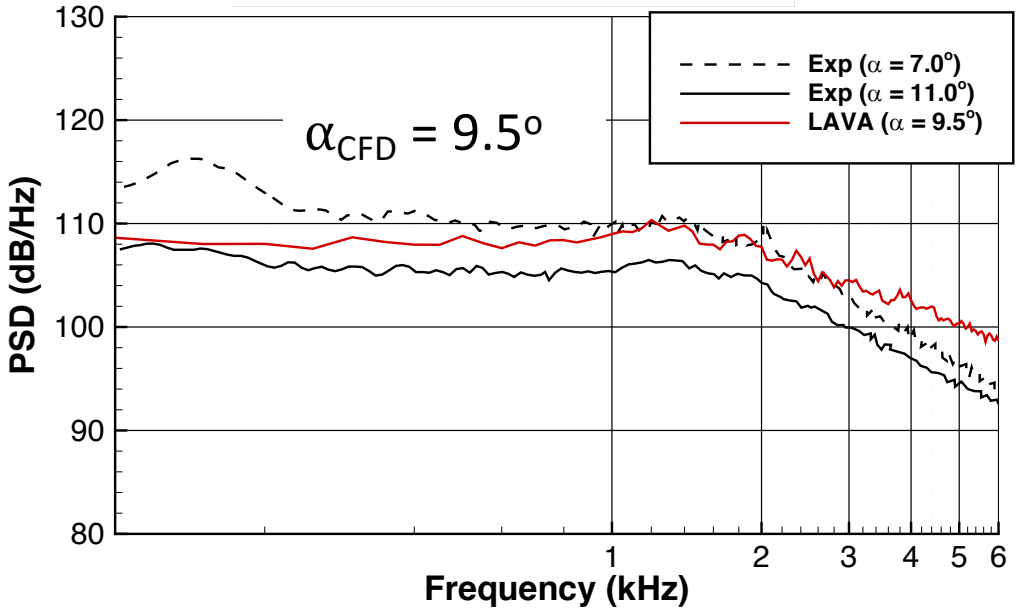

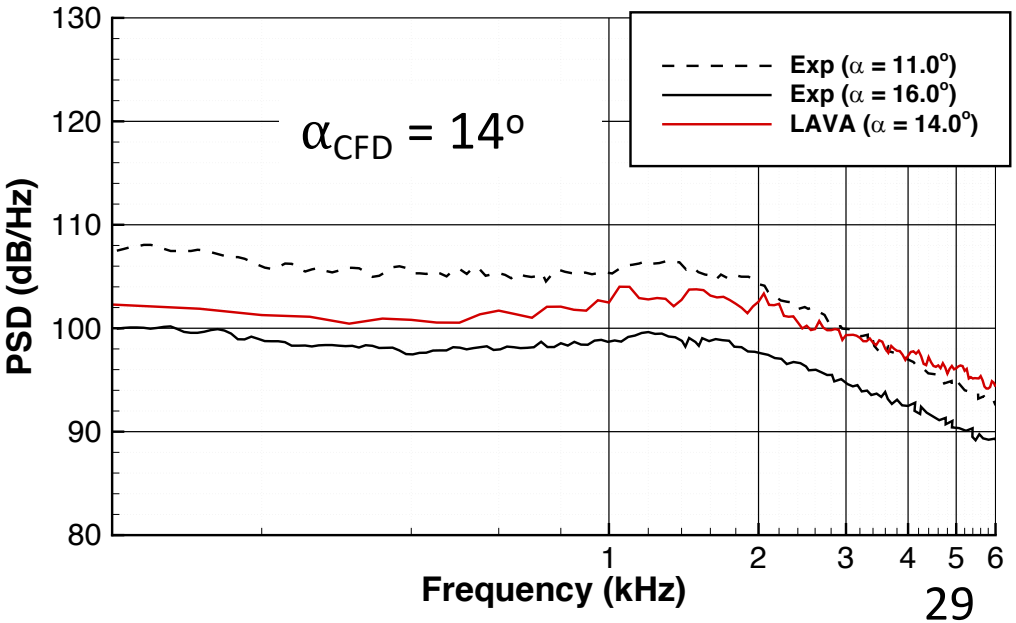

Near-Field Results

PSD at sensor location 8

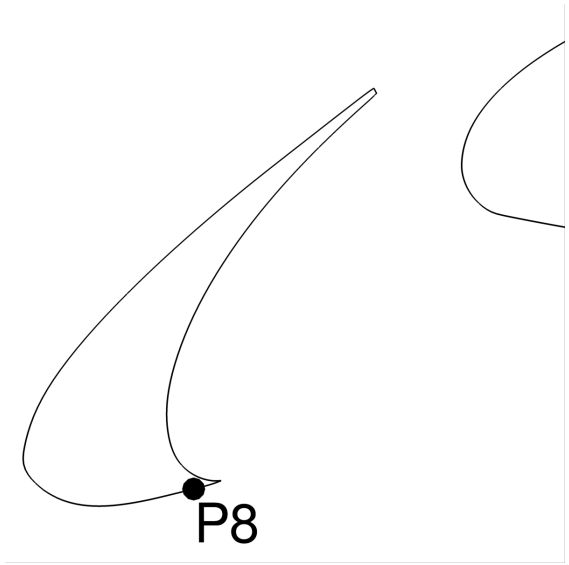

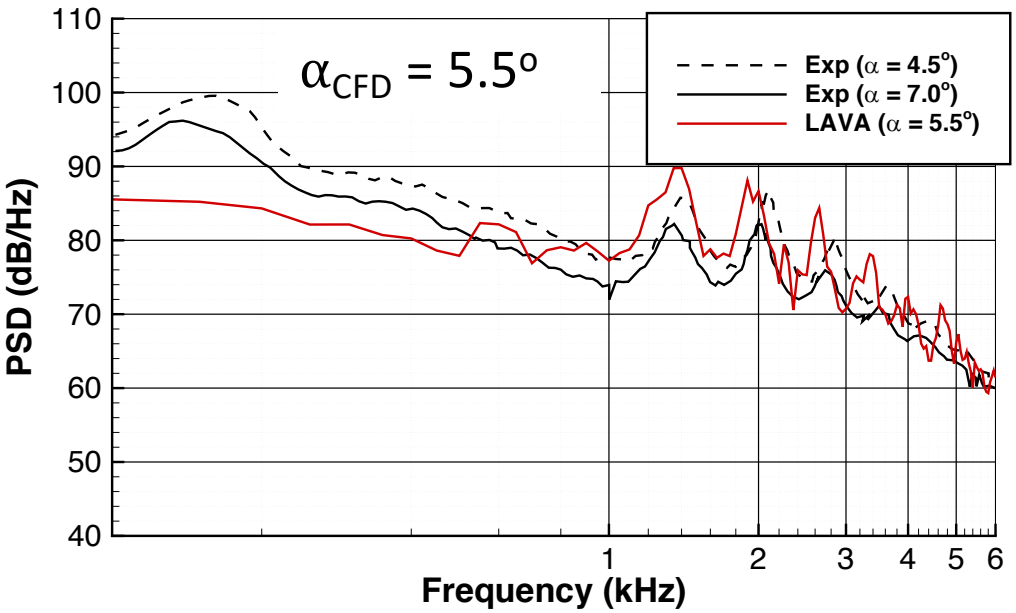

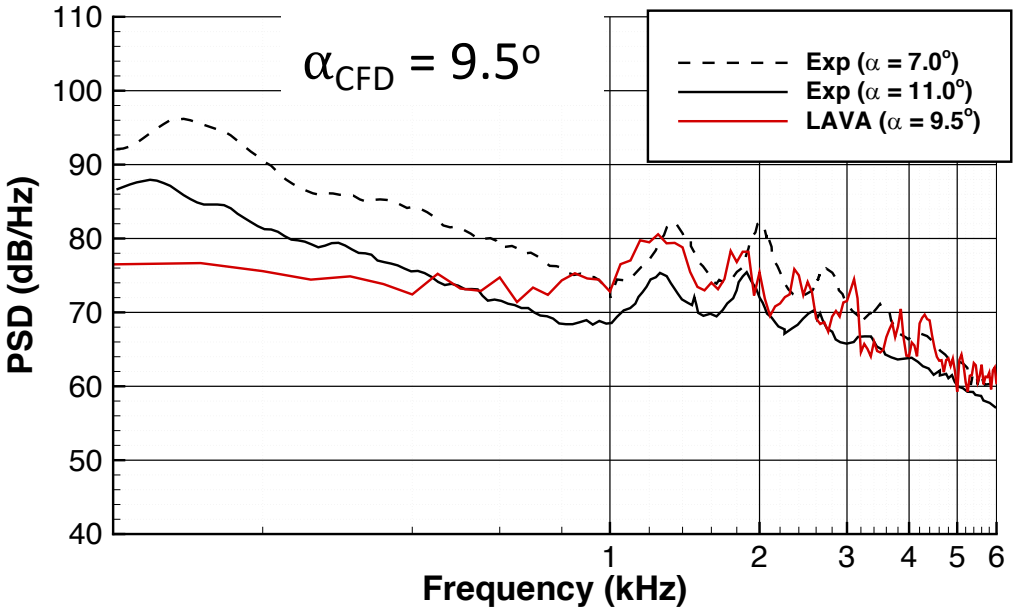

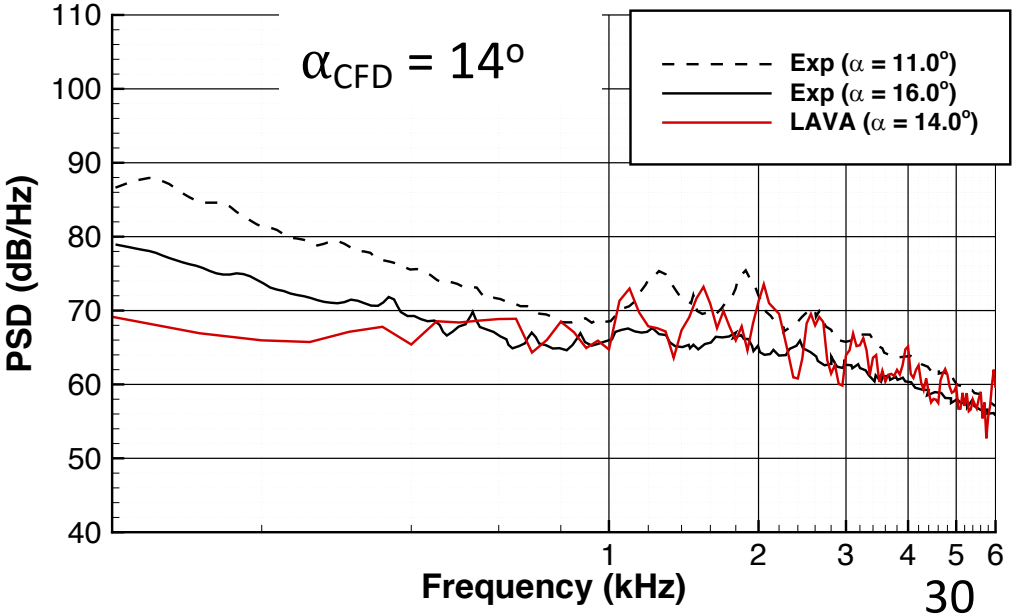

Near-Field Results

PSD at sensor location 9

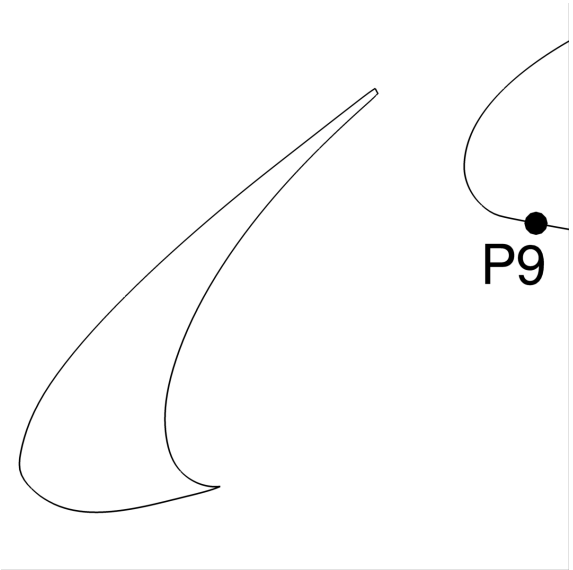

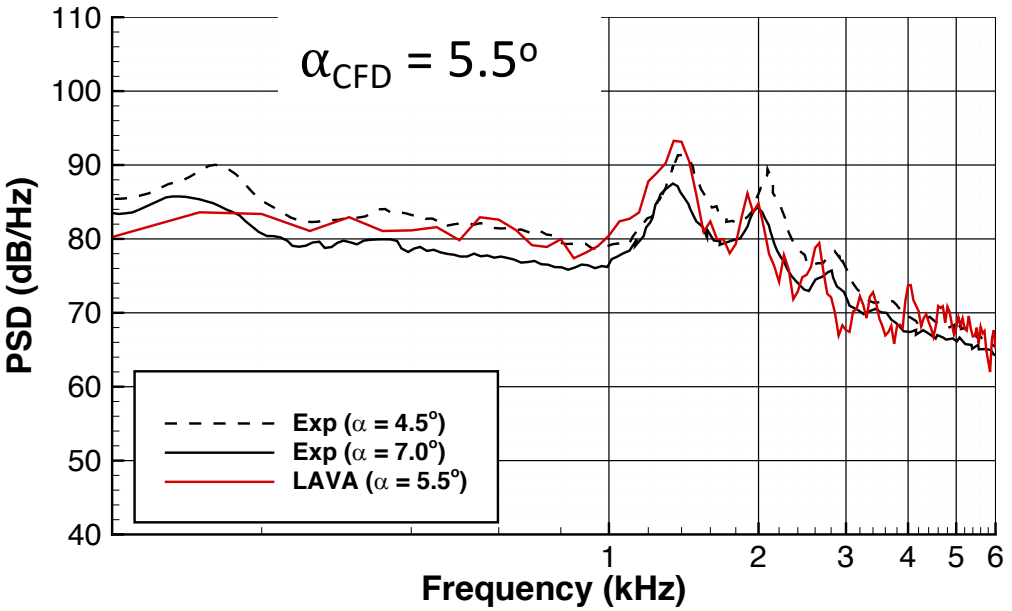

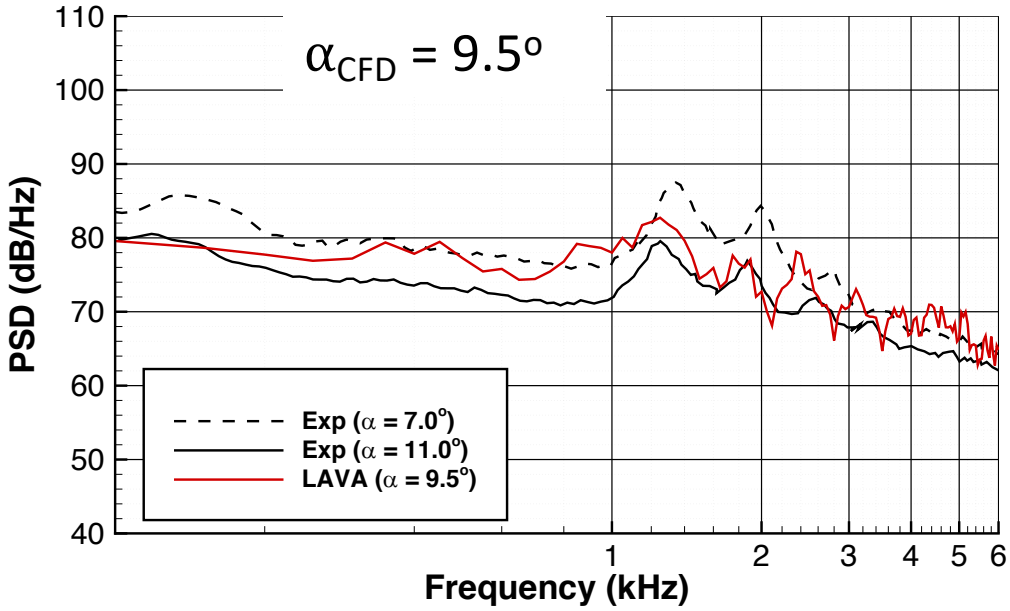

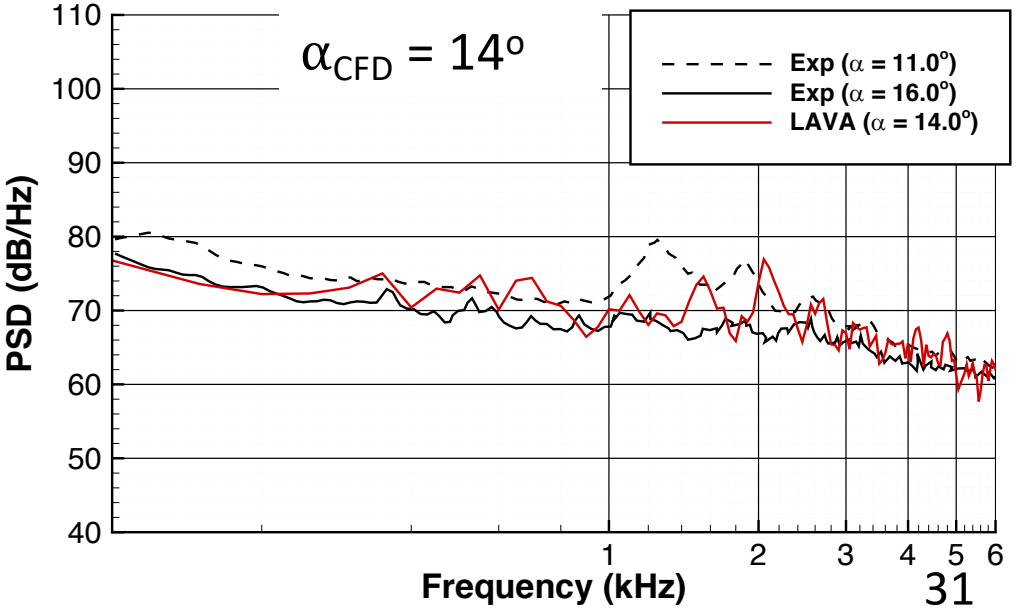

Near-Field Results

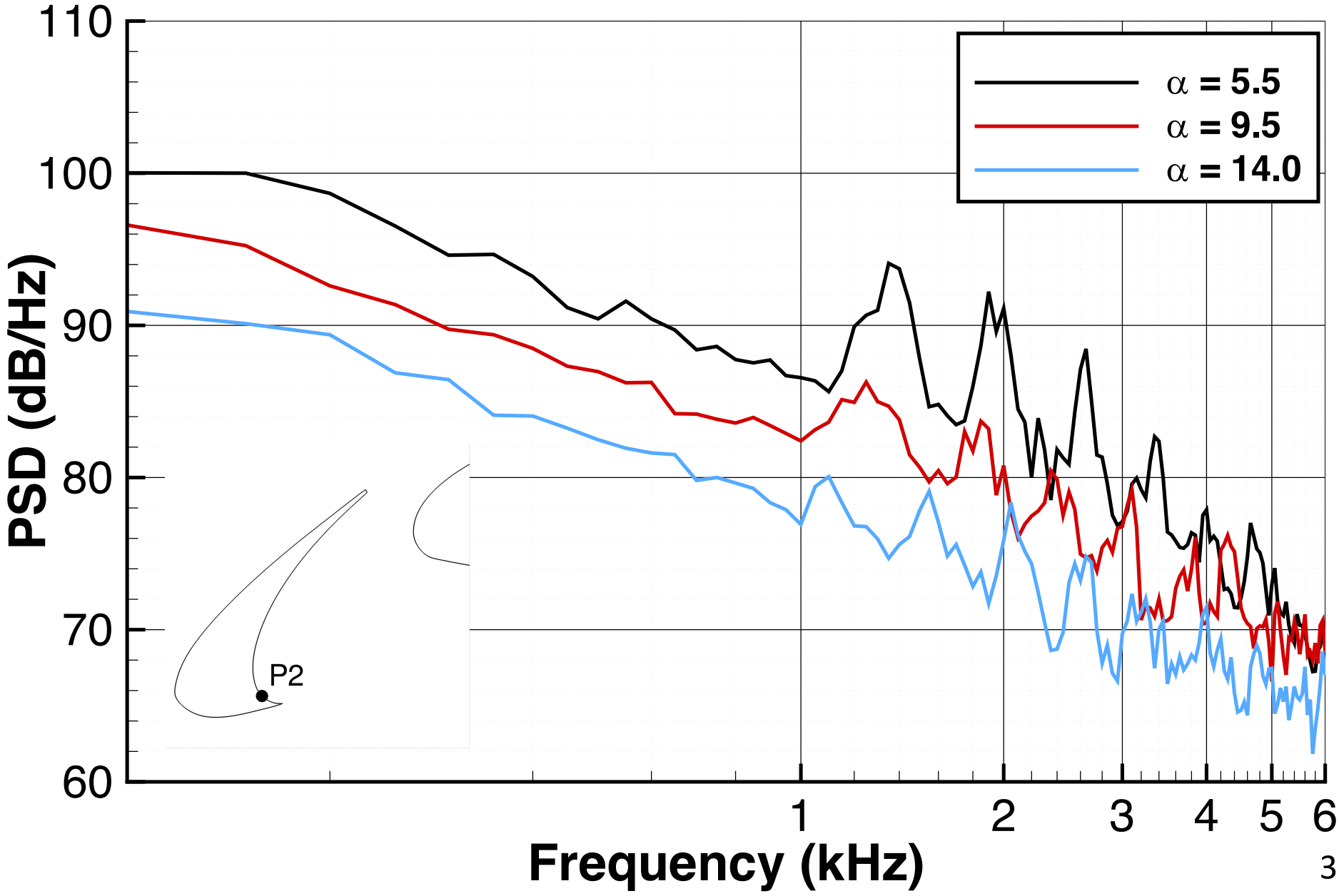

Near-Field Results

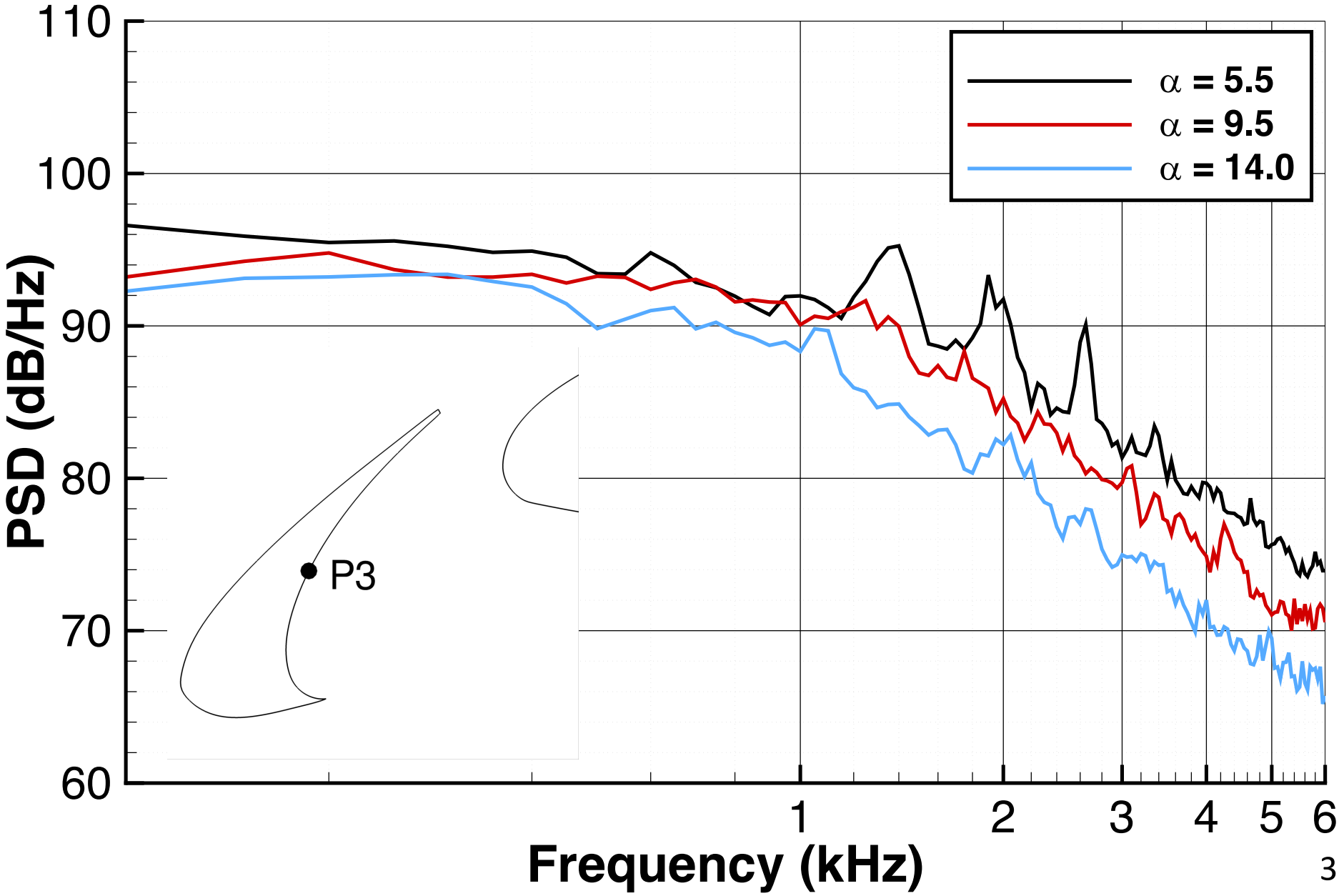

Near-Field Results

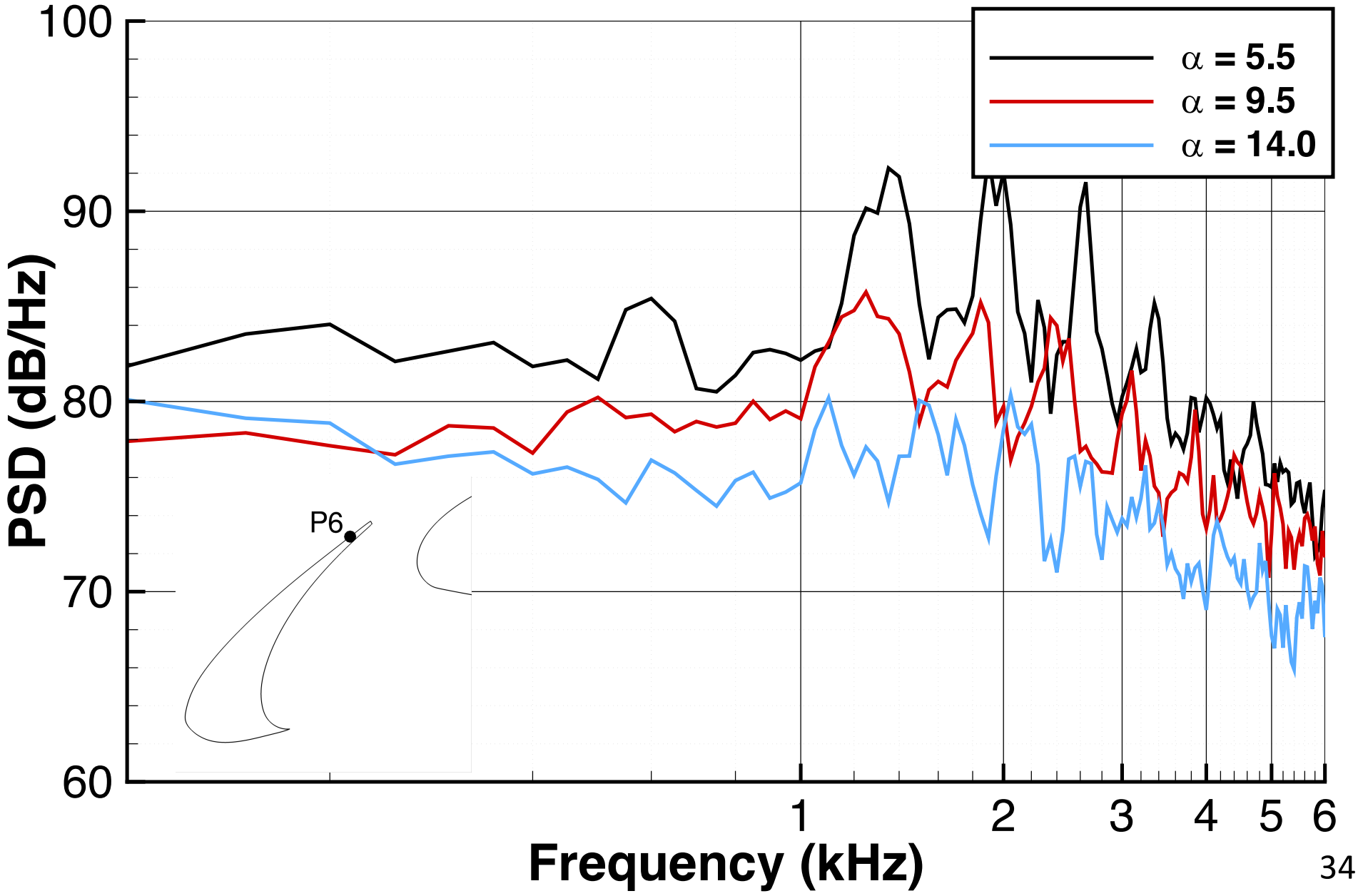

Near-Field Results

Contours of real part of pressure at narrow band peak 1, f = 1350 Hz

- Narrow Band Peak 1 (NBP1) appears to be a dipole generated in the slat cove
- Amplitude of pressure perturbations decrease with increasing AOA consistent with near-field PSD spectra
- Directivity pattern appears less sensitive to AOA compared to amplitude at this narrow band frequency

α=5.5º

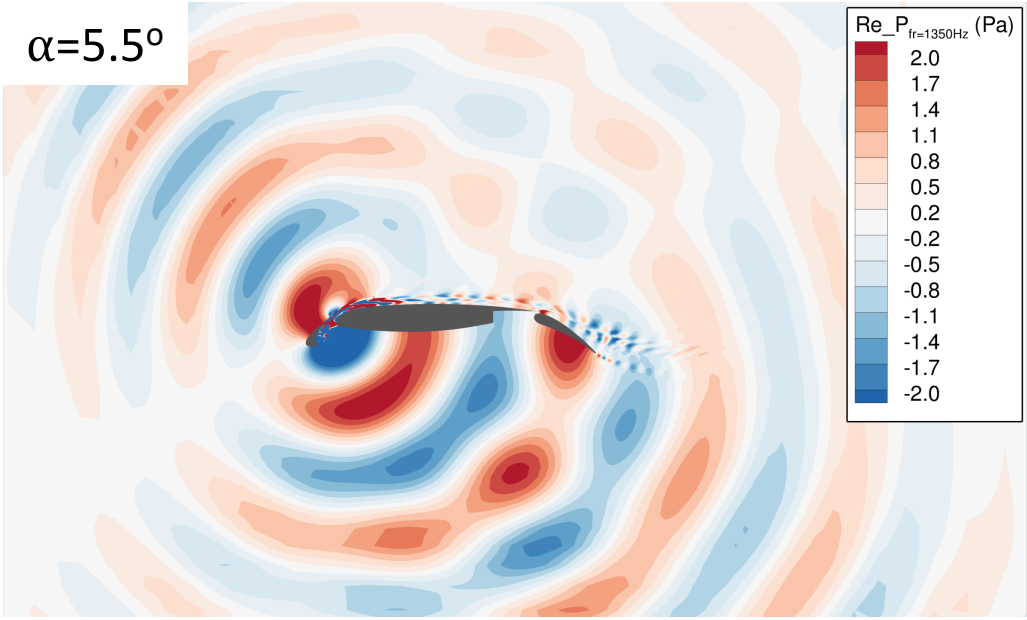

α=9.5º

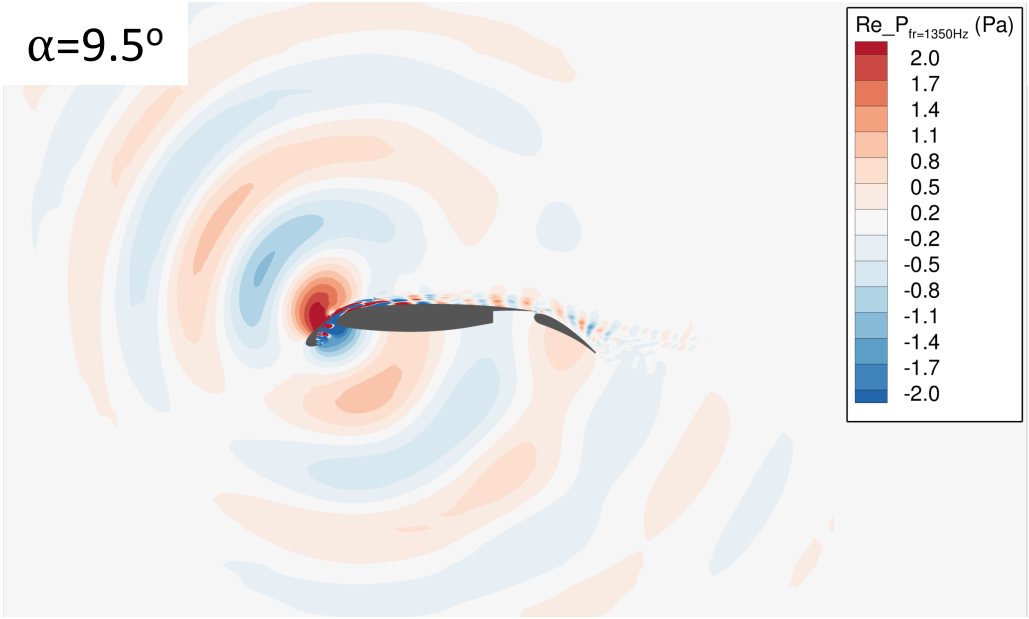

α=14.0º

Near-Field Results

Contours of real part of pressure at narrow band peak 2, f = 1900 Hz

- NBP2 is also predominantly a dipole, but show more geometric shielding effects at α=14.0º do to the smaller wave length
- Strong amplitude reduction with increasing AOA is observed at NBP2 similar to NBP1

α=5.5º

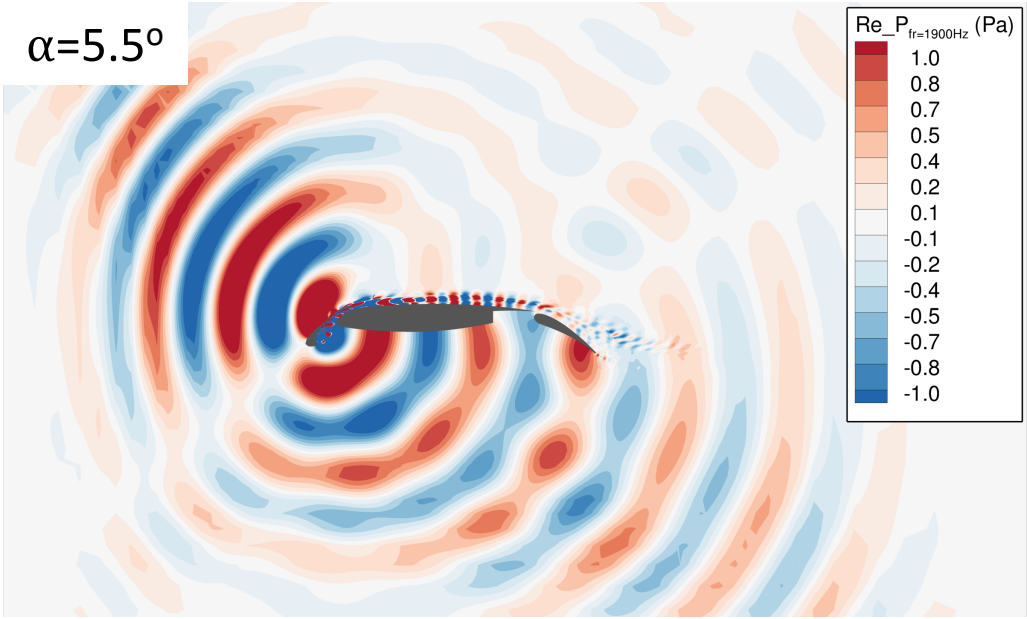

α=9.5º

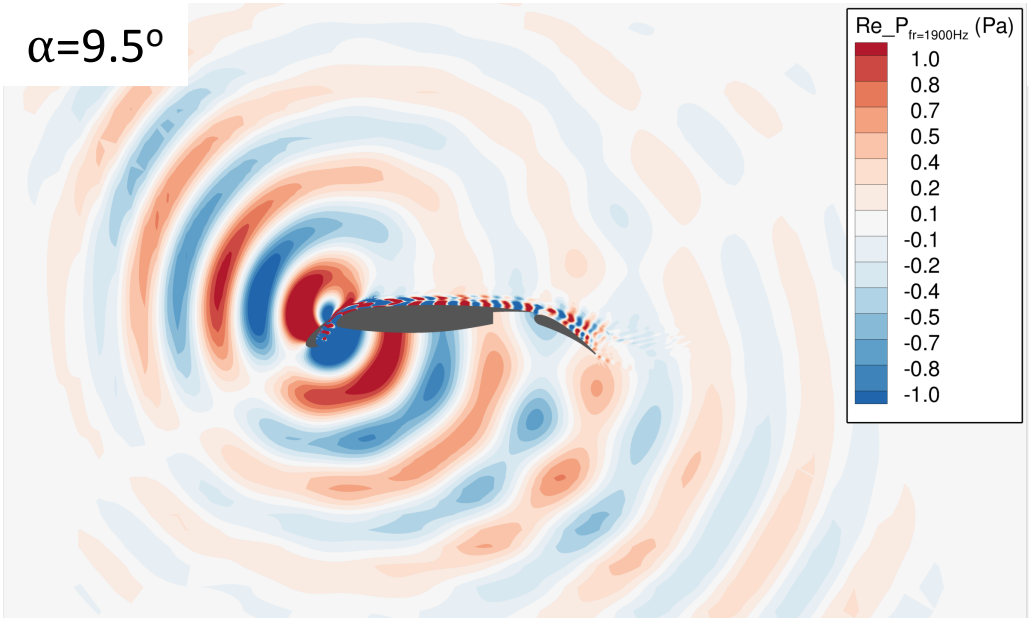

α=14.0º

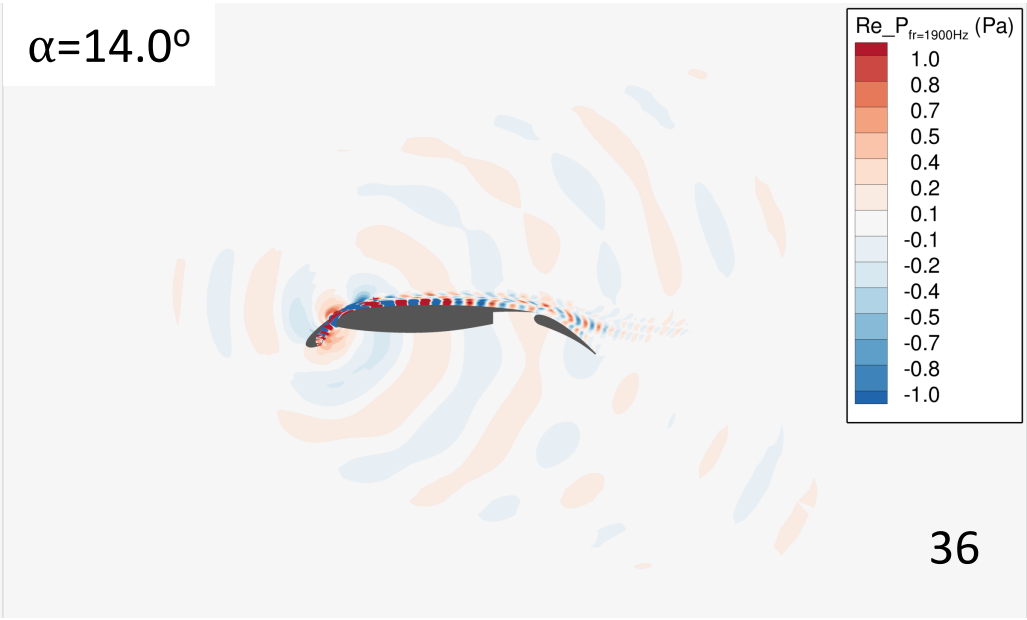

Far-Field Results

Ffowcs Williams-Hawkings (FWH) permeable (blue surface) and impermeable (airfoil surface) formulations used to propagate

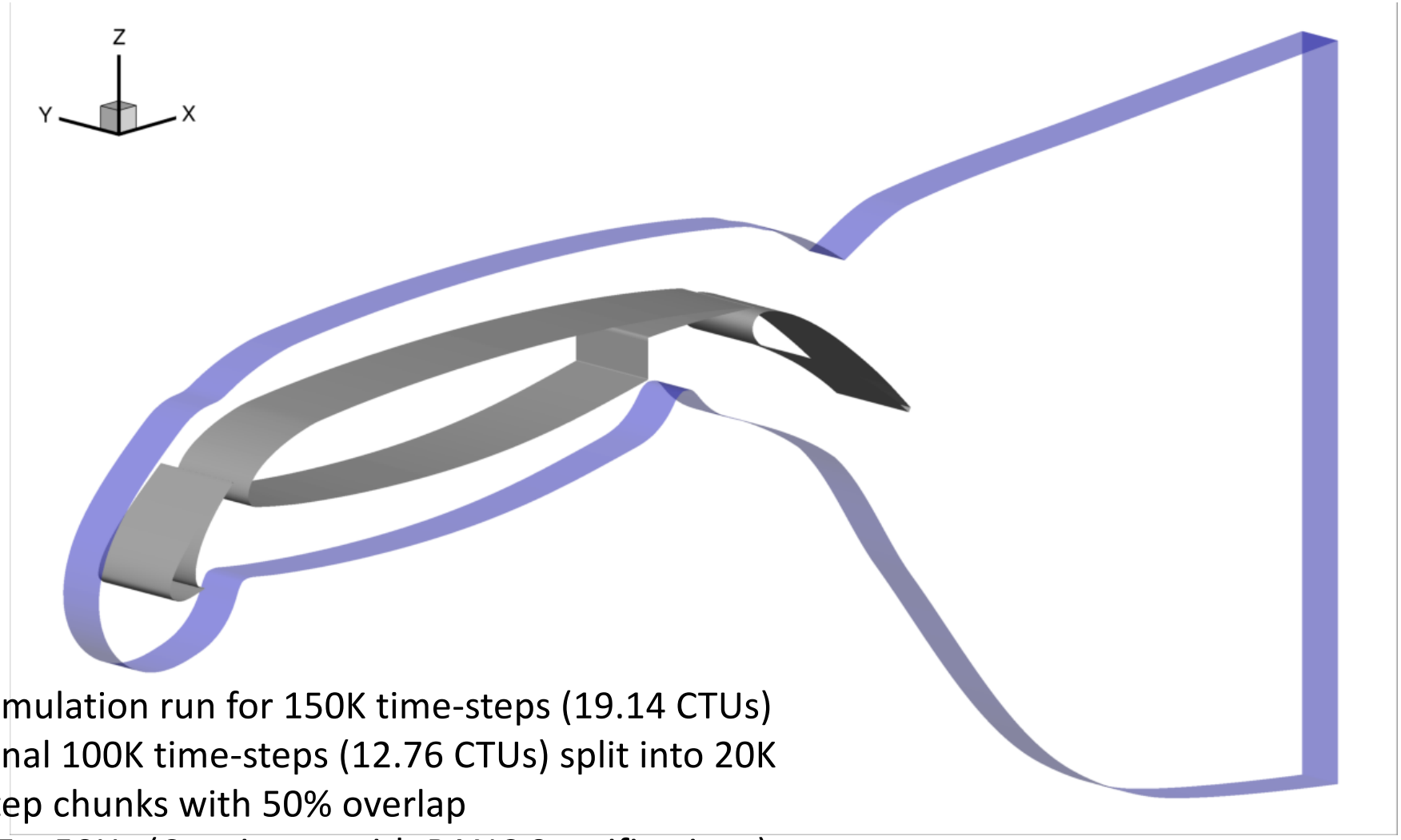

Simulation run for 150K time-steps (19.14 CTUs)
Final 100K time-steps (12.76 CTUs) split into 20K step chunks with 50% overlap
ΔF = 50Hz (Consistent with BANC Specifications)

Far-Field Results (10 Chords)

PSD for α_{CFD} = 5.5° (α_{WT} = 7.0°)

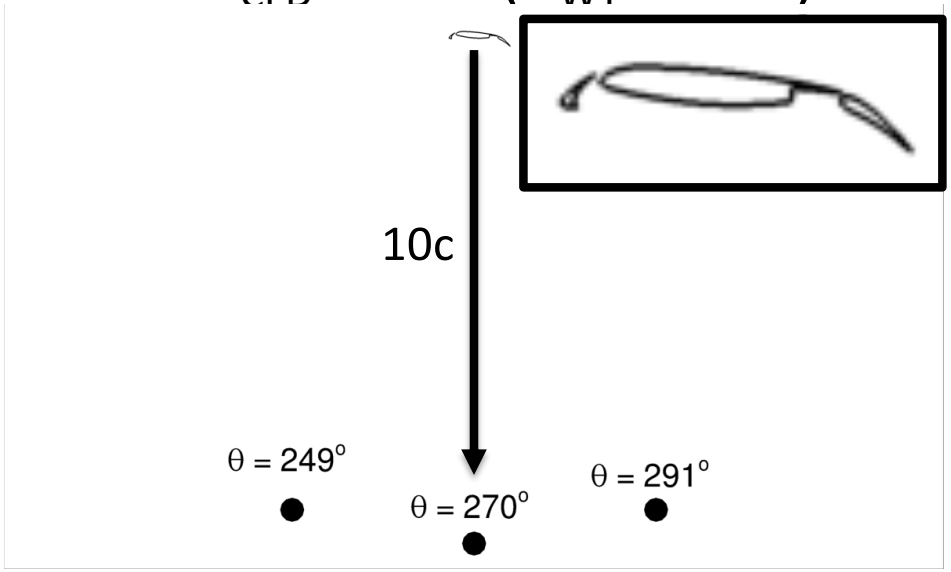

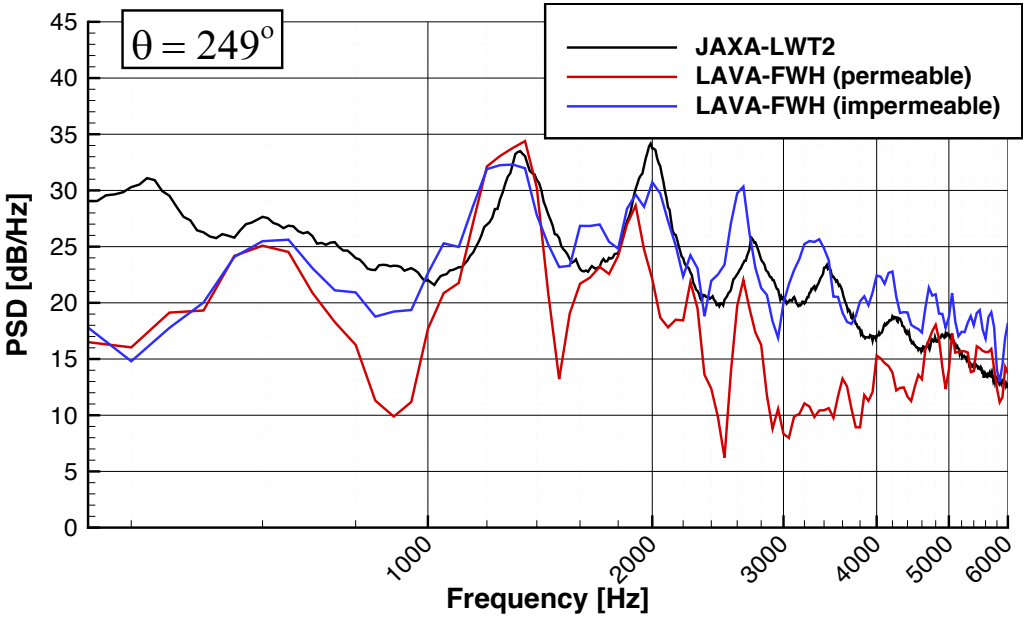

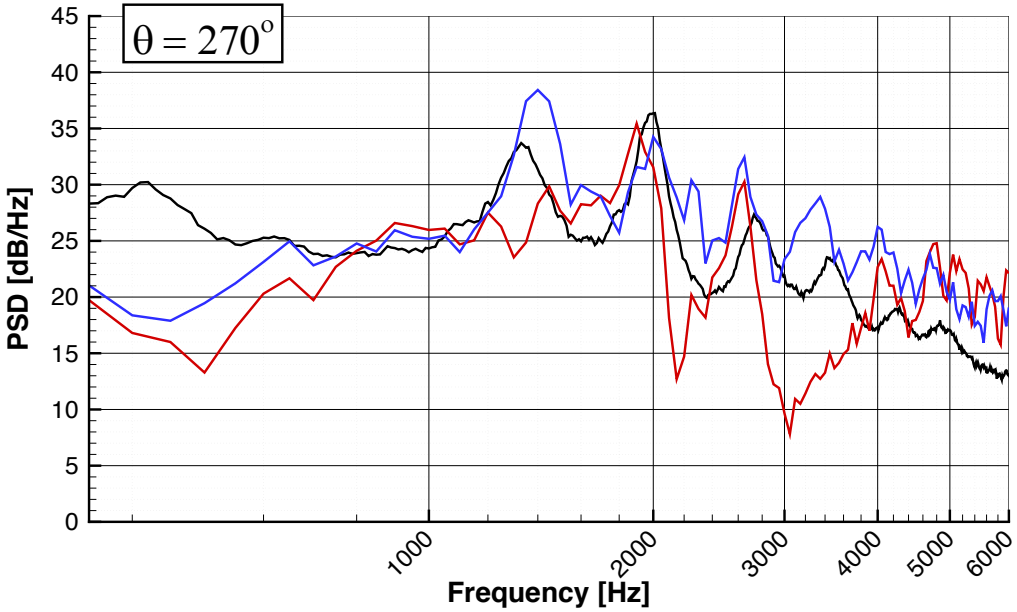

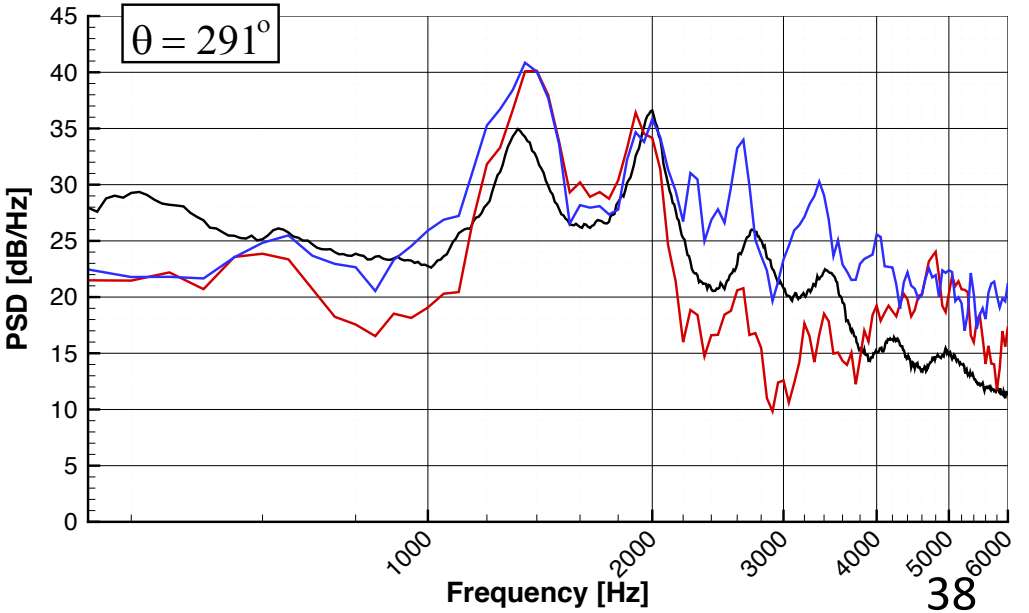

Far-Field Results (10 Chords)

PSD for α_{CFD} = 9.5° (α_{WT} = 11.0°)

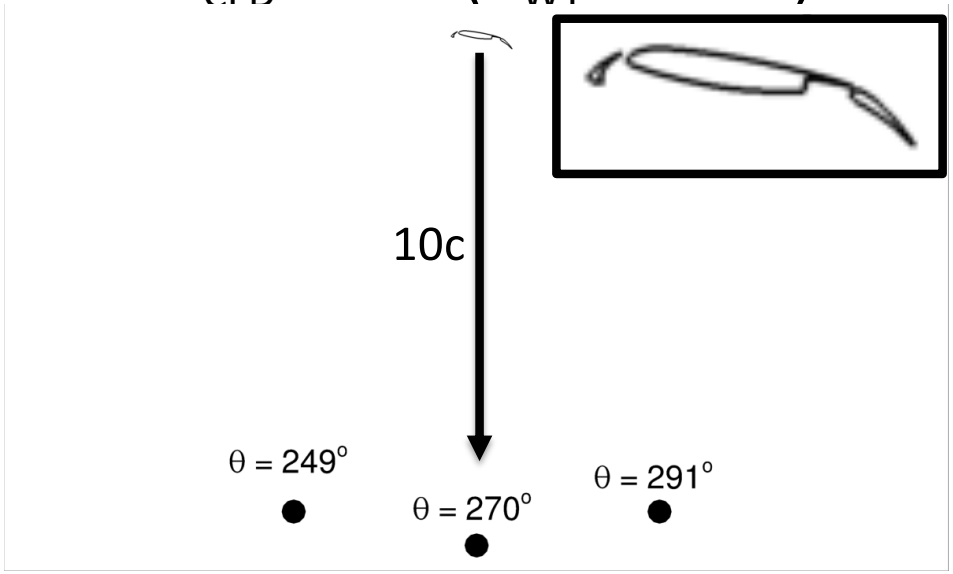

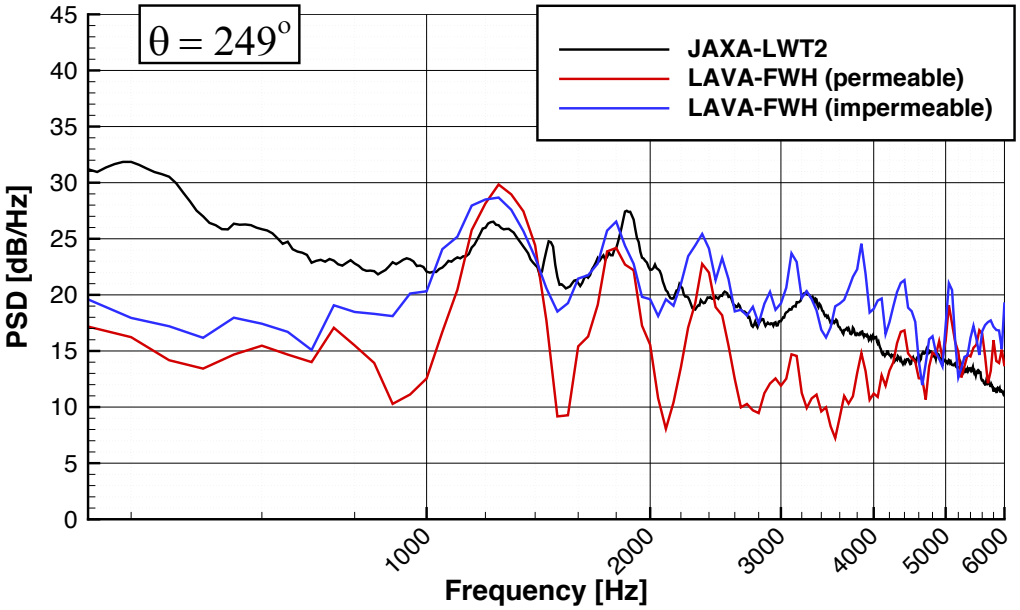

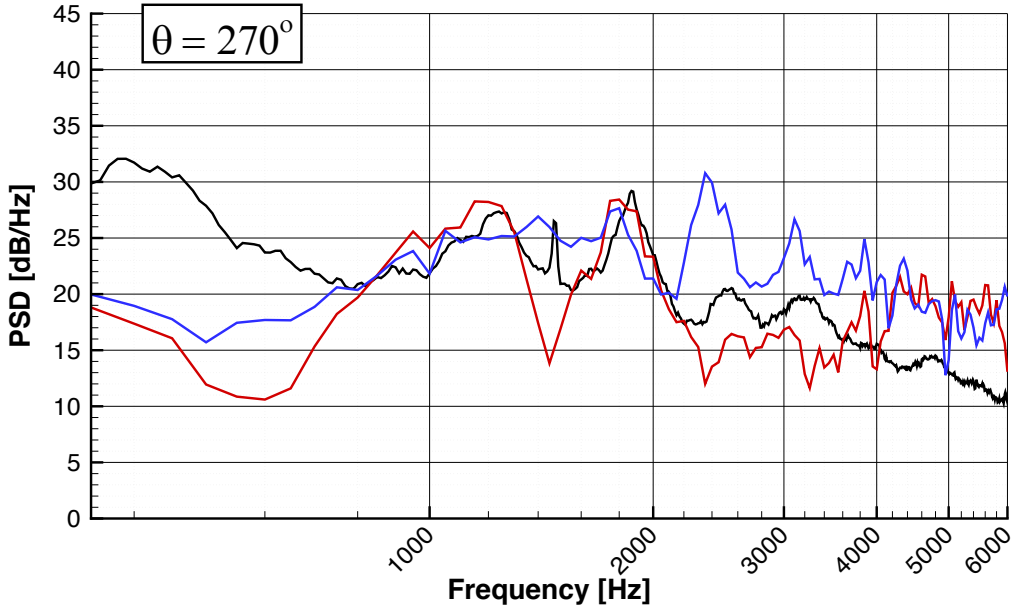

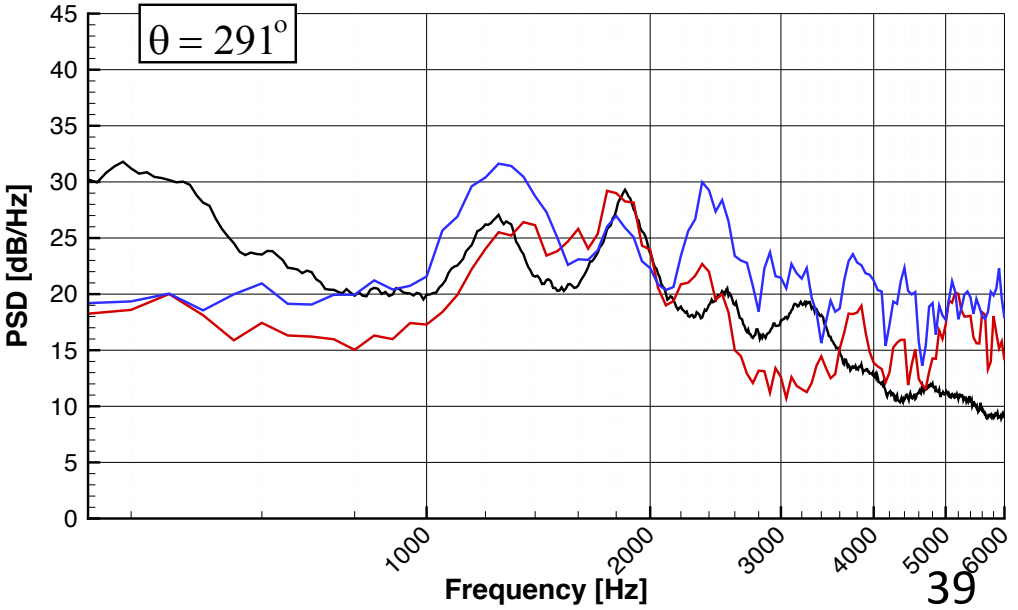

Far-Field Results (10 Chords)

PSD for α_{CFD} = 14.0° (α_{WT} = 16.0°)

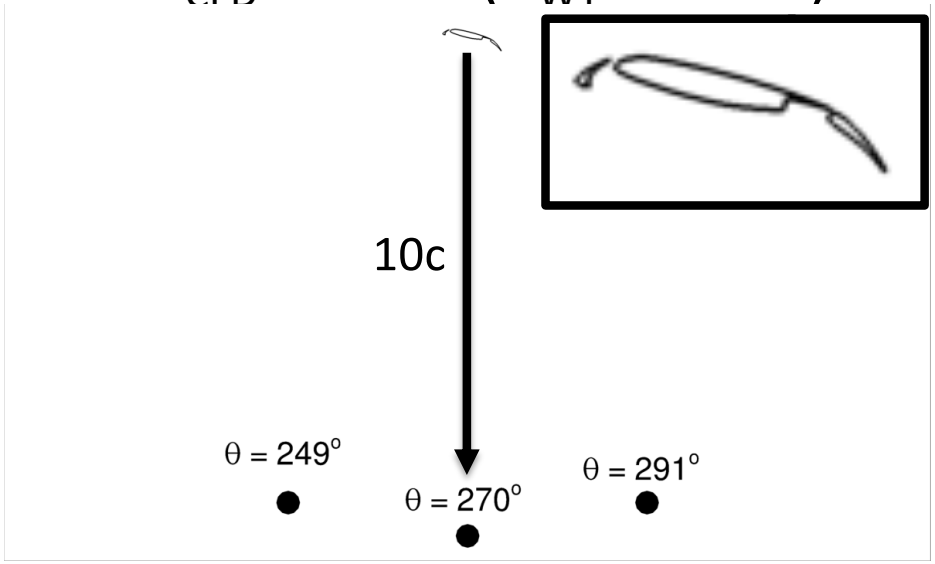

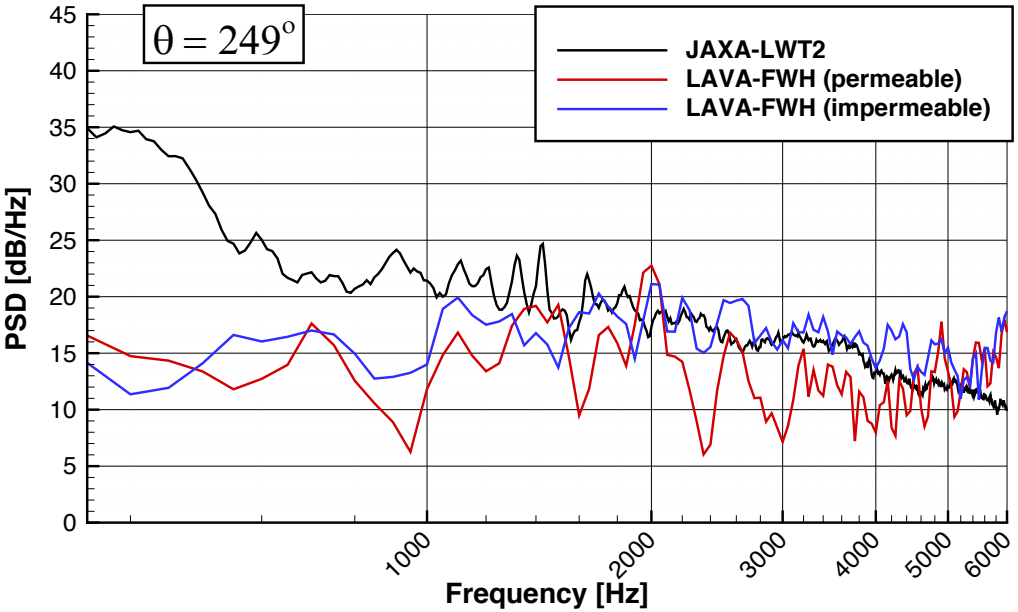

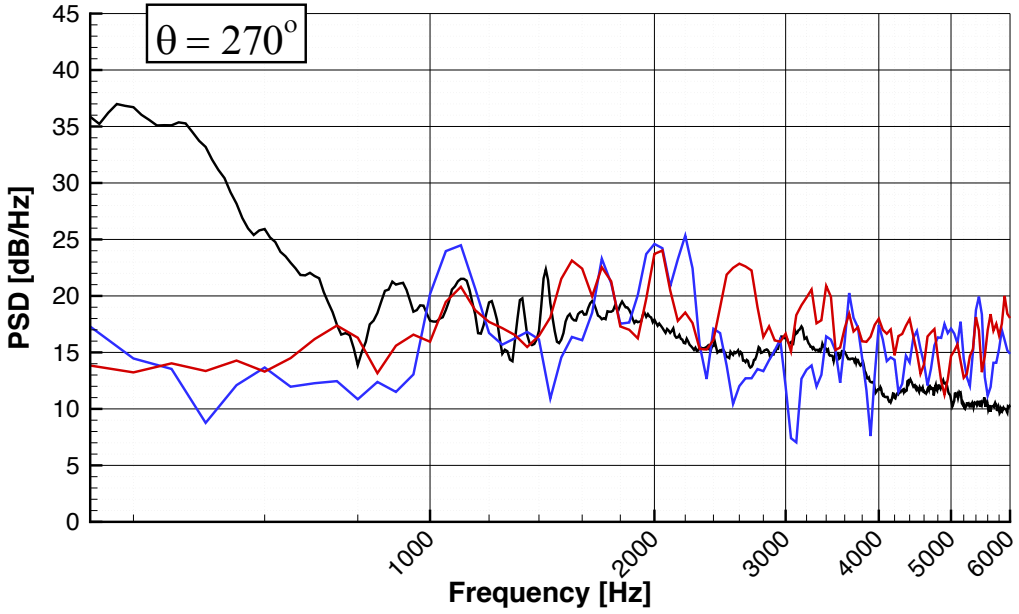

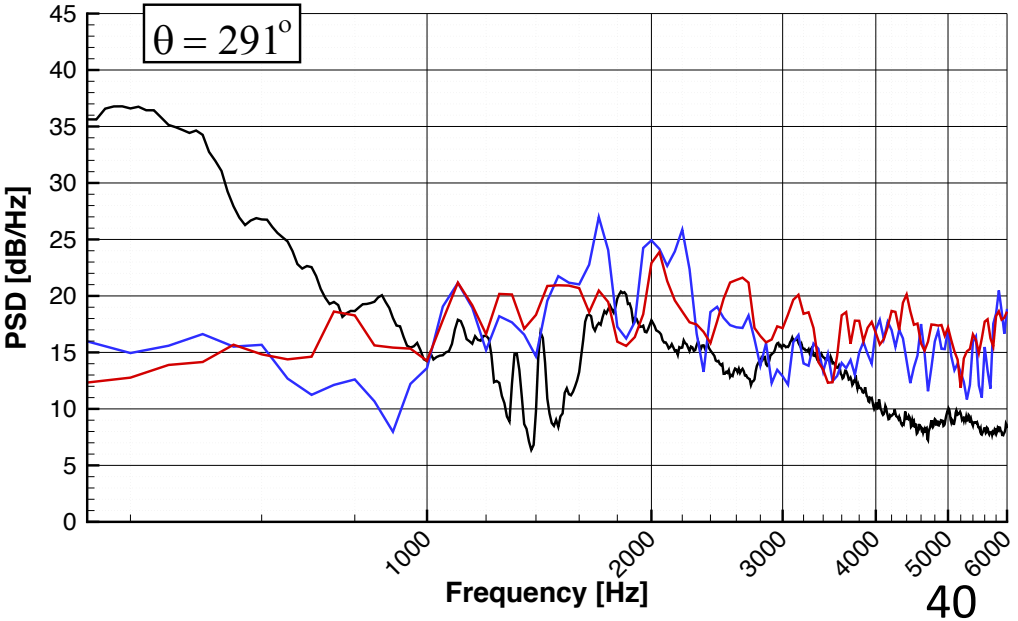

Far-Field Results

Sensitivity of PSD to angle of attack (impermeable)

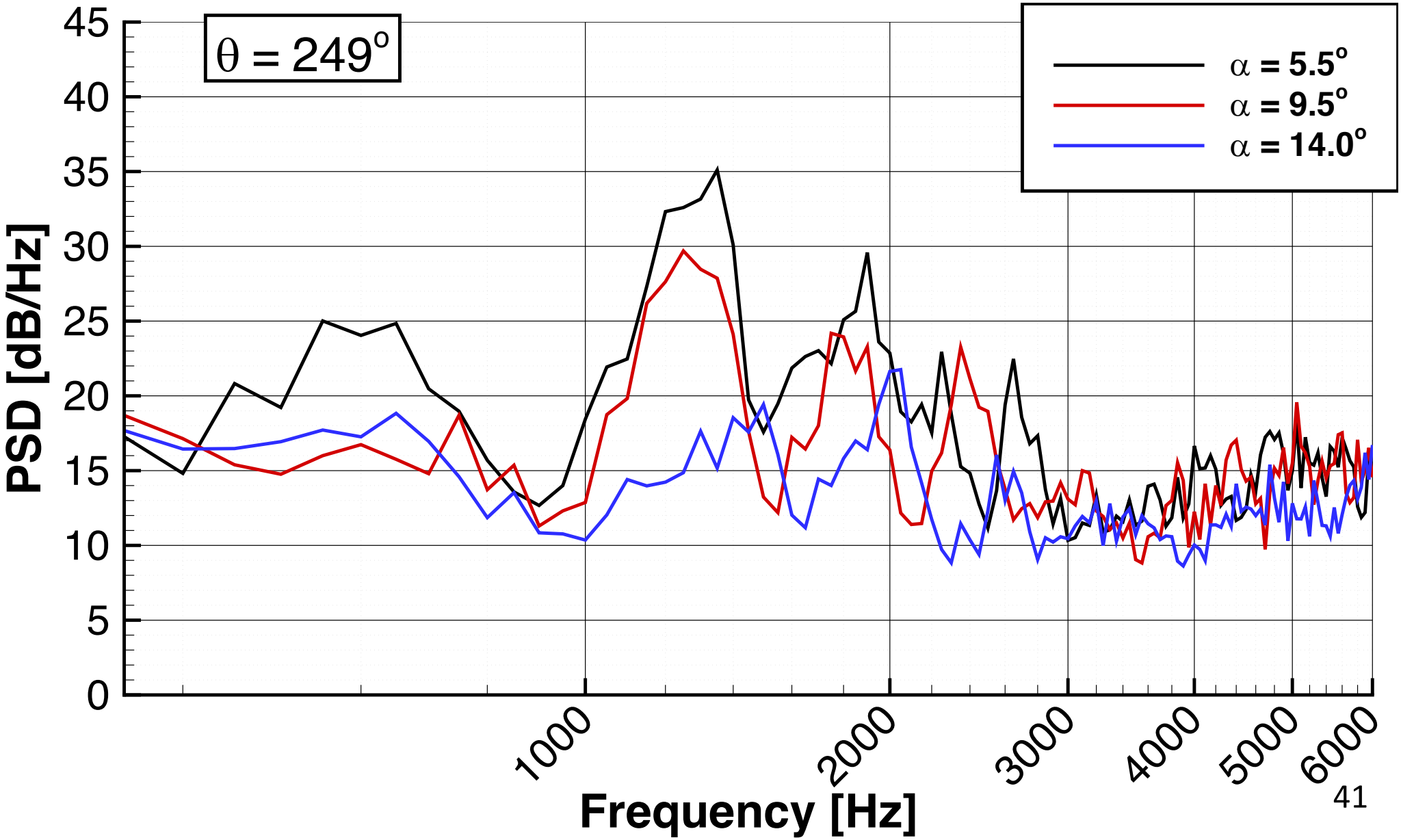

Far-Field Results

Sensitivity of PSD to angle of attack (impermeable)

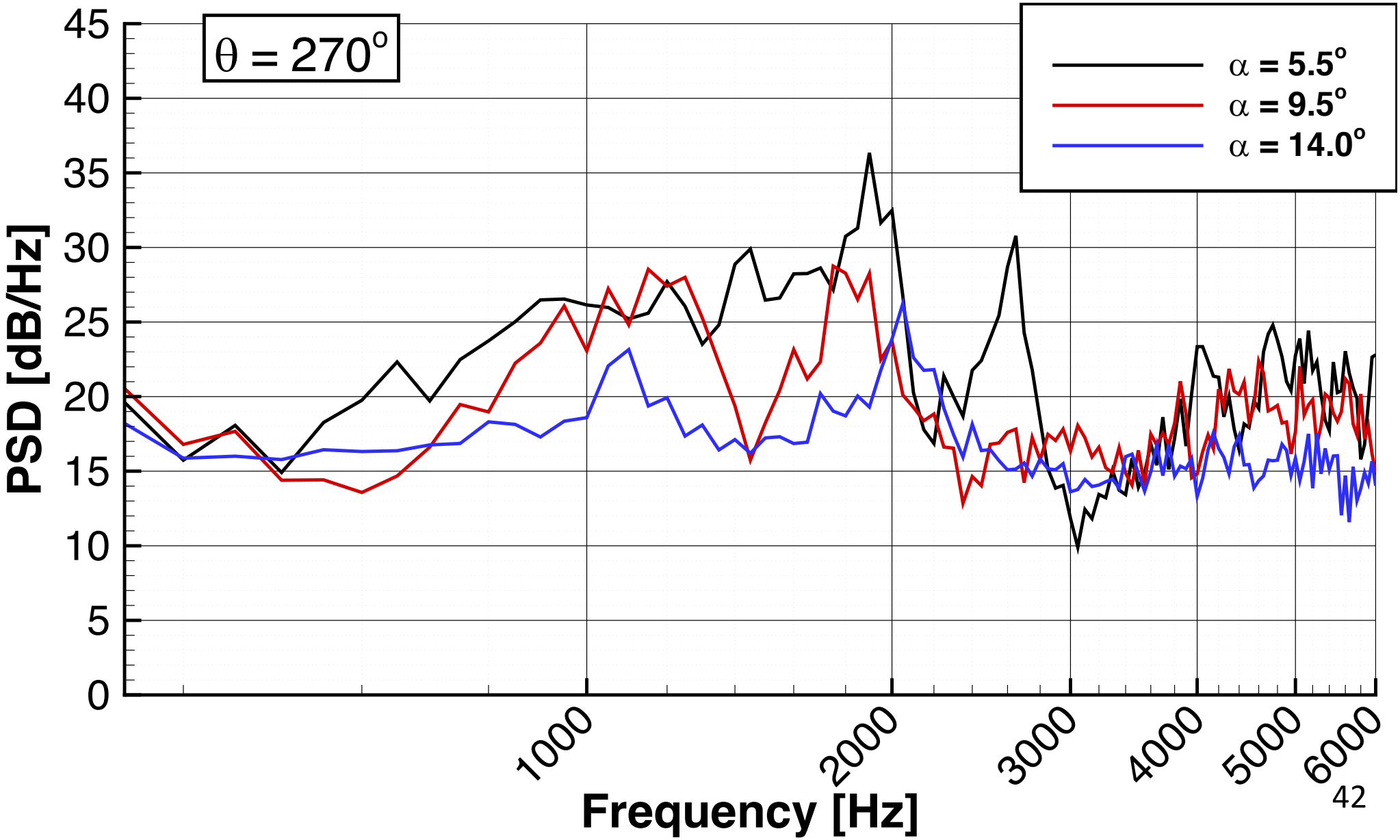

Far-Field Results

Sensitivity of PSD to angle of attack (impermeable)

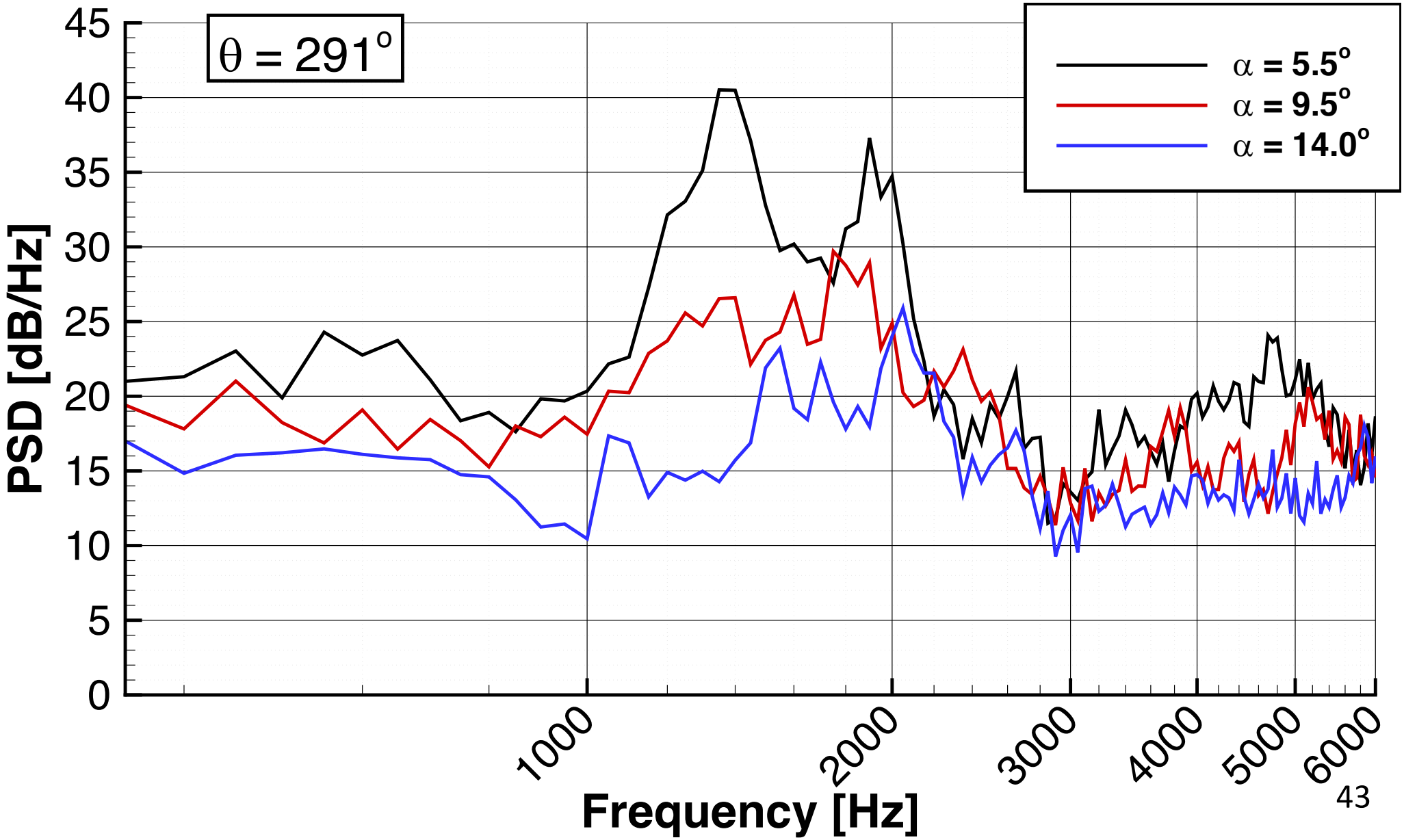

Far-Field Results

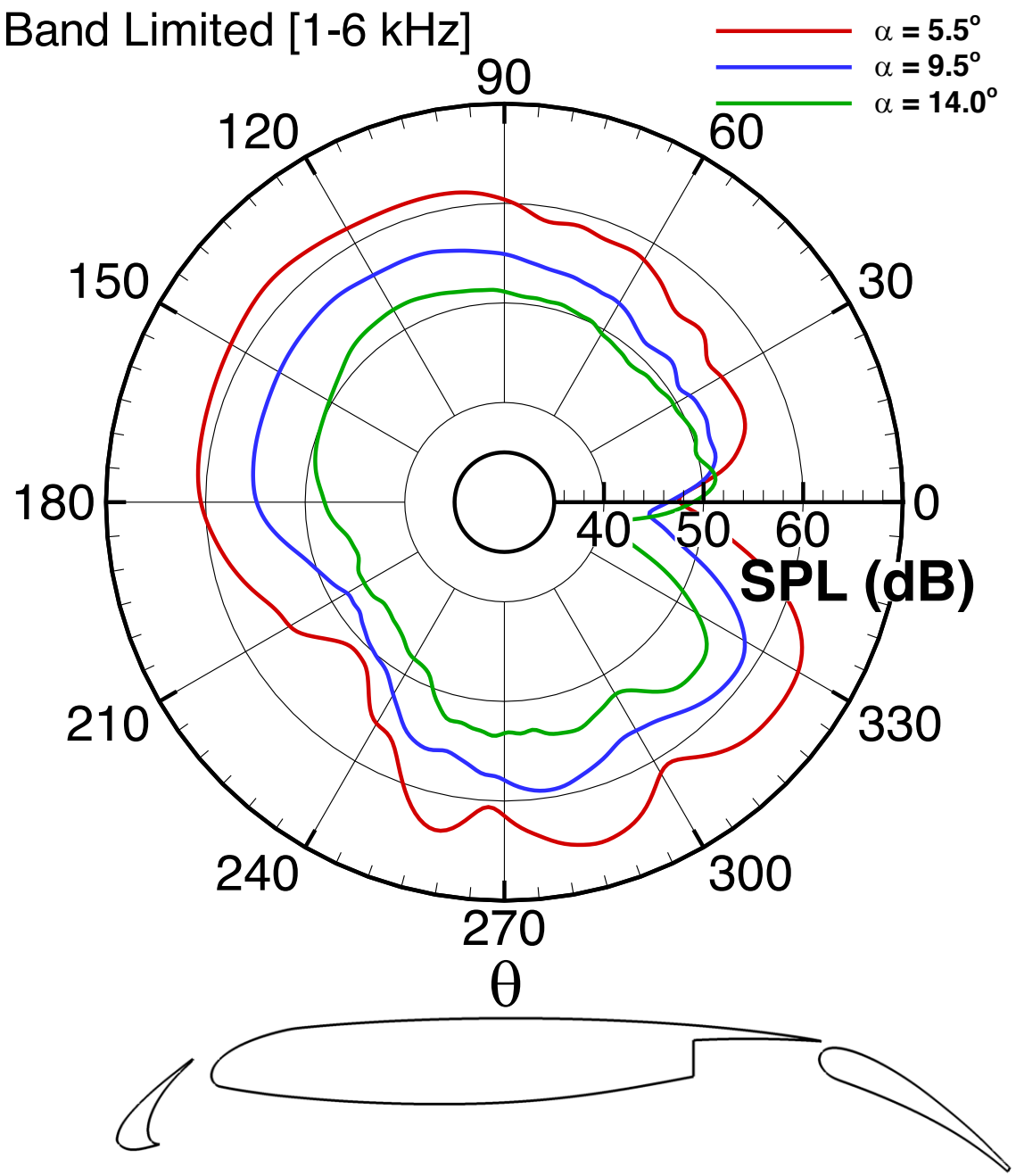

- Band Limited Overall Sound Pressure Level
  - Decrease in SPL with increasing AOA
  - Shift in directivity of low noise region from θ = 360° at α = 5.5° to θ = 350° at α = 14°
  - Shift in low noise region with increasing AOA caused by shielding of the slat cove region by the main element and flap
  - Lower SPL at 220° caused by shielding of slat cove by the slat itself

Summary

- ZDES has been successfully applied to predict aeroacoustic slat noise from the 30P30N high-lift system at high angles of attack
- Spatially varying spanwise grid spacing and zonal turbulence modeling resulted in an affordable approach to hybrid RANS-LES simulations
- Introduced Mode-4 (LES) for specialized shear-layer grids not explicitly attached to walls
- Good PSD comparisons with JAXA LWT2 Kevlar wall wind tunnel data obtained for both near-field and far-field measurements between 1-6 kHz

Summary

- Large discrepancy observed in far-field PSD levels below 1 kHz not found in the near-field comparisons
  1. Potentially caused by flap gap, flap, installation, or background noise (see 500 Hz noise maps reported in AIAA-2018-3460 *Murayama et. al.*)
  2. Length of time-interval window (ΔF = 50 Hz) maybe to small for the lower frequencies

- Three observations made for angle of attack effects on slat noise
  1) Reduction of narrow band peaks with increasing AOA
  2) Reduction in overall sound pressure levels with increasing AOA
  3) Shift in directivity of low noise region caused by shielding

- These results suggest that the ZDES method is mature enough to explore slat noise on more complicated configurations

Acknowledgements

- Work was funded by the NASA Aircraft Noise Reduction (ANR) sub-project under the Advanced Air Transport Technology (AATT) project and NASA's Transformative, Tools, and Technology (T^3) project
- Meelan Choudhari of NASA LaRC for organizing the Slat Noise Category of the AIAA Benchmark problems for Airframe Noise Computations (BANC) Workshop
- Movies created by Tim Sandstrom of NASA Ames
- Computer time has been provided by the NASA Advanced Supercomputing (NAS) facility at NASA Ames Research Center